

103

X-640-64-19

N 64 27251 lat. -32

TM X-55014

Code 1 NASA TMX-55014

SHADES OF EGO

S-49

BY

H. E. MONTGOMERY
S. J. PADDACK
F. B. SHAFFER

JANUARY 1964



— GODDARD SPACE FLIGHT CENTER —
GREENBELT, MD.

OTS PRICE

XEROX

\$

9.10 ph

MICROFILM

\$

SHADES OF EGO

S-49

by

H. E. Montgomery

S. J. Paddack

F. B. Shaffer

Theoretical Division
Goddard Space Flight Center
Greenbelt, Maryland

ACKNOWLEDGMENT

The authors wish to acknowledge the support and constructive criticism of R. K. Squires and the members of the Special Projects Branch of the Theoretical Division. Dr. H. Wolf of Analytical Mechanics Associates (under contract to Goddard Space Flight Center, contract number NAS 5-2535) originally conceived the analyses presented in sections IV and V of this report. These analyses were combined with the ITEM Program (Reference 1) in order to generate the results. The total program has developed over a period of several years; consequently, it is impossible to mention all of those who have contributed.

ABSTRACT

27251

This report presents shadow data and heat input data for the S-49 EGO. It gives times for which each experiment is in the shadow of either the Earth, the satellite's main box or the solar array. It also gives the heat inputs to the experiments as a function of time from launch for one complete orbit. The heat inputs include direct solar radiation, reflected solar radiation and Earth emitted radiation.

The shadow data are presented for a launch date of May 15, 1964 at 13.0 hours U.T. The heat input data are for a launch time of May 15, 1964 at 8.0 hours U.T. The injection elements are from Reference 2. The satellite's geometry is from References 3 and 4.

Author

TABLE OF CONTENTS

	<u>Page</u>
I. INTRODUCTION	1
II. NOTATION	3
III. ASSUMPTIONS	12
A. INITIAL CONDITIONS	12
B. RESTRAINTS ON LAUNCH TIME	12
C. S-49 SPACECRAFT GEOMETRY	12
IV. MATHEMATICAL MODEL FOR SHADOW TESTING . . .	16
A. GENERAL DESCRIPTION OF THE SHADOW COMPUTATIONS	16
B. AN EXPERIMENT SHADOWED FROM THE SUN BY A POLYGONAL PLANE FACE	17
C. IDEAL CONTROL LAWS AND DEFINITION OF AXES SYSTEMS	26
D. DETAILED SHADOW TESTING PROCEDURE	32
V. MATHEMATICAL MODEL FOR HEAT INPUTS TO AN ARBITRARILY ORIENTED SURFACE OF OGO	37
A. DIRECT SOLAR RADIANT HEAT	37
B. REFLECTED SOLAR RADIANT HEAT	38
C. EARTH EMITTED RADIANT HEAT	44

	<u>Page</u>
VI. RESULTS AND DISCUSSION	46
A. SHADOW STUDY	46
B. HEAT INPUTS	49
VII. REFERENCES	56
APPENDIX A	A-1
APPENDIX B	B-1
APPENDIX C	C-1
APPENDIX D	D-1

I. INTRODUCTION

The Orbiting Geophysical Observatory (OGO) consists of a main box, the solar array and the orbital plane experiment package (OPEP). Experiments may be appended to any of the three main component parts either directly or on booms. As many as fifty experiment packages may be carried on the OGO spacecraft. (See Figure 1). The solar array and the OPEP may rotate relative to the main box. The main box and the solar array are considered as casting shadows and carrying experiments, the OPEP is considered only as carrying experiments. A method for calculating the radiant heat inputs to each experiment is also presented in this report. These inputs include direct solar, reflected solar and Earth emitted heat flux. If an experiment is shielded from the Sun by the Earth, the main box or the solar array, the solar input to that particular experiment is set to zero. If an experiment is in the eclipse of the Earth the reflected solar (as well as the direct solar) heat input is set equal to zero. However, the effects of shadowing of an experiment from the Earth by the main box or the solar array is not considered in the computation of the solar reflected or Earth emitted heat inputs to that particular experiment. Shadow data are presented for the S-49 (EGO) for a launch date of May 15, 1964 at 13.0 hours U.T. The heat input data are for a launch time of May 15, 1964

at 8.0 hours U.T. The injection elements are from Reference 2. The S-49 geometry is from References 3 and 4.

181745

II. NOTATION

A Cross sectional area.

a The fraction of the solar constant σ which is reflected away from the Earth (albedo).

a_E The equatorial radius of the Earth.

$f_a(\gamma_1, \gamma_2, \gamma_3, r)$ The integrand of the integral for $\dot{q}_{na}(t)$. In equation (47) it is defined on page 38.

$f_E(\gamma_2, \gamma_3, r)$ The integrand of the integral for $\dot{q}_{nE}(t)$. In equation (60) it is defined on page 44.

$f(i)$ Incidence factor defined by equation (45).

$\bar{H} \equiv \bar{r}_{VE} \times \dot{\bar{r}}_{VE}$; the angular momentum vector per unit mass.

$I(t)$ Shadow indicator at time t ; 0 in shadow, 1 not in shadow.

i Angle of incidence.

$\bar{i}, \bar{j}, \bar{k}$ Orthogonal unit vectors.

$\bar{L}_{j,j+1} \equiv (a, b, c)$; the 3-vector representing the line connecting the projections of points j and $j + 1$ onto a test plane, as defined by equations (20, 21), and appendix C.

$\bar{l}_j, j + 1 \equiv \bar{p}_{j+1}'' - \bar{p}_j''$; as used in appendices C and D.

\bar{N}_{l_m} Outward normal to an elemental area ΔA_{l_m} of the Earth's surface; it is defined in equation (49).

\bar{n} Unit vector normal to an experiment surface.

\bar{P}_i Augmented position vector $(x_i'', y_i'', 1)$.

\bar{p}_i'' A position vector (x_i'', y_i'') defined by equation (17).

\bar{Q}_n Augmented position vector $(x_n'', y_n'', 1)$.

\bar{q}_n'' A position vector (x_n'', y_n'') defined by equation (18).

\bar{q} A position vector used in appendix B.

$\dot{q}_{nE}(t)$ The heat flux incident upon a surface of the n^{th} experiment at time t , which is emitted by the Earth. It is given by equations (60) and (62).

q_{nE} The accumulated heat flux \dot{q}_{nE} over a time interval; it is defined by equation (63).

$\dot{q}_{na}(t)$ The heat flux incident upon a surface of the n^{th} experiment at time t , which originates at the Sun and reflects from the Earth. It is defined by equations (47) and (58).

q_{na} The accumulated heat flux $\dot{q}_{na}(t)$ over a time interval; it is defined by equation (59).

$\dot{q}_{ns}(t)$ The heat flux incident upon a surface of the n^{th} experiment at time t , which radiates directly from the Sun. It is defined by equation (43).

q_{ns} The accumulated heat flux \dot{q}_{ns} over a time interval; it is defined by equation (46).

\bar{R} Augmented position vector $(x, y, z, 1)$, (a 4-vector).

\bar{r} A position vector (x, y, z) .

\bar{r}_{VE} The vector which points from the Earth to the vehicle.

$\dot{\bar{r}}_{VE}$ The velocity of the vehicle relative to the Earth.

\bar{r}_{lm} The vector which points from the satellite to the Earth's elemental surface area ΔA_{lm} . It is given by equation (51).

\bar{r}_{sv} The vector which points from the vehicle to the Sun.

\bar{r}_{slm} The vector which points from the Earth's elemental surface area ΔA_{lm} to the Sun.

\bar{r}_{se} The vector which points from the Earth to the Sun.

$\bar{S}_i \equiv (A_i, B_i, C_i, D_i)$; a 4-vector representing a face defined in equation (3).

s Defined by equation (10).

t Time.

t_o Reference time.

$\bar{U} \equiv (1, 1, 1)$; a vector.

u Defined by equation (22).

$\bar{X}_{lmn}, \bar{Y}_{lmn}, \bar{Z}_{lmn}$ Vectors (x_l, x_m, x_n) , (y_l, y_m, y_n) and (z_l, z_m, z_n) , respectively.

x, y, z The coordinate system associated with $\bar{i}, \bar{j}, \bar{k}$, respectively.

α The angle corresponding to the longitude in the plane normal to \bar{r}_{VE} , the zero line being the projection of \bar{i}_B on this plane. (See Figure 5).

α_m The value of α associated with the elemental area ΔA_{lm} ; defined by equation (50).

β The angle between \bar{r}_{VE} and the tangent to the Earth from the satellite; (equation 48).

γ_1 The angle of incidence of the Sun's rays on an elemental area of the Earth's surface.

γ_{1lm} The value of γ_1 associated with the elemental area ΔA_{lm} . It is the angle between the vectors \bar{N}_{lm} and \bar{r}_{slm} (Figure 5). It appears in equation (52).

γ_2 The angle between the radius vector which points from an elemental area of the Earth's surface to the vehicle and the normal to that area.

- γ_{2l_m} The value of γ_2 associated with the elemental area ΔA_{l_m} . It is the angle between the vectors \bar{N}_{l_m} and $(-\bar{r}_{l_m})$ (Figure 5). It appears in equation (54).
- γ_3 The angle between the vector which points from the vehicle to an elemental area of the Earth's surface and the unit outward normal to the experiment surface.
- γ_{3l_m} The value of γ_3 associated with ΔA_{l_m} . It is the angle between the vectors \bar{n} and \bar{r}_{l_m} (Figure 5). It appears in equation (55).
- ΔA_{l_m} An incremental surface area of the Earth (Figure 5); it is defined in equation (57).
- θ The angle between the vector \bar{r}_{vE} and the radius vector from the center of the Earth to the surface element in question.
- θ_l The value of θ associated with the elemental area ΔA_{l_m} . It is the angle between \bar{N}_{l_m} and \bar{r}_{vE} . Equation (50).

Λ The emittance per unit area of the surface of the Earth.

σ The solar constant

Φ The solar array angle; defined by equation (35).
(Figure 1).

Ψ The OPEP angle; defined by equation (42). (Figure 1).

Superscripts and Subscripts

Denotes rotated coordinates in equations (4), (5), (7), (8) and (9). Also denotes a change of origin location in equations (14) and (15).

" Denotes vectors in the test plane.

B Box.

n Referring to the n^{th} experiment.

p Solar array.

p_o Referring to a point on the solar array axis.

T OPEP.

T_o Referring to a point on the OPEP axis.

Vector Operations

$\bar{\mathbf{A}} \times \bar{\mathbf{B}}$ The cross product of the vectors $\bar{\mathbf{A}}$ and $\bar{\mathbf{B}}$.

$\bar{\mathbf{A}} \cdot \bar{\mathbf{B}}$ The scalar product of vectors $\bar{\mathbf{A}}$ and $\bar{\mathbf{B}}$.

$\nabla F \equiv \bar{\mathbf{i}} \frac{\partial F}{\partial x} + \bar{\mathbf{j}} \frac{\partial F}{\partial y} + \bar{\mathbf{k}} \frac{\partial F}{\partial z}$; the gradient of the scalar function F .

III. ASSUMPTIONS

A. Initial Conditions

The initial conditions are assumed to be the same as the Agena burnout conditions (Reference 2) namely:

geocentric latitude	= -20.28 degrees
terrestrial longitude	= 111.902 degrees
geocentric height	= 281621.6 meters
the speed of the vehicle	= 10645.27 meters per second
azimuth	= 66.355 degrees
flight path angle	= 1.47148 degrees

B. Restraints on Launch Time

The results presented in this report are for launch times for which perigee does not go below its initial value for one year. See Reference 5 for the results of a detailed launch window study.

C. S-49 Spacecraft Geometry

The assumed geometry, presented in this section, is given in the box coordinate system. The center of gravity (c.g.) of the spacecraft was arbitrarily chosen as the origin. The coordinates of the solar paddles and the OPEP are given in a standard position relative to the box (solar array angle $\phi = 0$ and OPEP angle $\psi = 0$) together with the location of their axes of rotation.

1. Shadowing Surfaces

a. Main Box — The box coordinates of the vertices (corners) of the main box are as follows: (See Figure 2).

<u>Point</u>	<u>x</u> <u>inches</u>	<u>y</u> <u>inches</u>	<u>z</u> <u>inches</u>
1	-14.607	23.5	14.983
2	-14.607	-43.5	14.983
3	14.607	-43.5	14.983
4	14.607	23.5	14.983
5	-14.607	23.5	-14.983
6	-14.607	-43.5	-14.983
7	14.607	-43.5	-14.983
8	14.607	23.5	-14.983

b. Solar Array — The coordinates of the solar array are as follows: (See Figure 2).

<u>Point</u>	<u>x</u> <u>inches</u>	<u>y</u> <u>inches</u>	<u>z</u> <u>inches</u>
P1	-117.841	0.0	-36.877
P2	-117.841	0.0	36.877
P3	- 39.541	0.0	36.877
P4	- 39.541	0.0	18.677
P5	- 26.491	0.0	18.677
P6	- 26.491	0.0	-18.677

<u>Point</u>	<u>x</u> <u>inches</u>	<u>y</u> <u>inches</u>	<u>z</u> <u>inches</u>
P7	- 39.541	0.0	-18.677
P8	- 39.541	0.0	-36.877
P9	117.841	0.0	-36.877
P10	117.841	0.0	36.877
P11	39.541	0.0	36.877
P12	39.541	0.0	18.677
P13	26.491	0.0	18.677
P14	26.491	0.0	-18.677
P15	39.541	0.0	-18.677
P16	39.541	0.0	-36.877

The axis of rotation of the solar array passes through the point

$$(x_{p_0}, y_{p_0}, z_{p_0}) = (0, 0, 0).$$

2. Experiments

The coordinates of the experiments and their normals are as follows (See Figure 2).

<u>COORDINATES</u>			
<u>Experiment</u>	<u>x</u> <u>Inches</u>	<u>y</u> <u>Inches</u>	<u>z</u> <u>Inches</u>
E.P. 1	- 74.2	91.1	12.3
E.P. 2	49.9	100.1	15.3
E.P. 3	- 12.7	103.1	- 4.2

<u>Experiment</u>	<u>x</u> <u>Inches</u>	<u>y</u> <u>Inches</u>	<u>z</u> <u>Inches</u>
E.P. 4	20.6	- 94.4	-19.2
E.P. 5	11.4	288.1	-25.2
E.P. 6	- 6.7	-288.9	-16.7
SOEP 1	-102.7	3.4	- .30
SOEP 2	102.4	3.4	- .30
OPEP 1	- .2	43.1	45.8
OPEP 2	- .2	43.1	-45.8

The axis of rotation of the OPEPS passes through the point

$$(x_{T_o}, y_{T_o}, z_{T_o}) = (0, 43.5, 0).$$

<u>Normals</u>	<u>x</u>	<u>y</u>	<u>z</u>
E.P. 1	-1.0	0.0	0.0
E.P. 2	0.0	1.0	0.0
E.P. 3	0.0	1.0	0.0
E.P. 4	0.0	-1.0	0.0
E.P. 5	0.0	1.0	0.0
E.P. 6	0.0	-1.0	0.0
SOEP 1	0.0	1.0	0.0
SOEP 2	0.0	1.0	0.0
OPEP 1	1.0	0.0	0.0
OPEP 2	1.0	0.0	0.0

IV. MATHEMATICAL MODEL FOR SHADOW TESTING

A. General Description of the Shadow Computations

In order to carry out the shadow computations, the geometry of the satellite (the main box, the solar array, and the experiments) has to be described analytically. The configuration of the satellite is described in a coordinate system which is fixed in the main box. The shadowing of experiments by the main box and the solar array is determined by testing the shadow cast by each of their component faces. This may result in some duplicate testing, since part of the faces may overlap, but no special assumption need be made as to its shape. Any three dimensional object may be approximately described by a number of plane faces.

The geometry of the satellite is input to the program by loading the coordinates of all its vertices and identifying the vertices belonging to each component face. Care must be taken that the polygon circumscribing each component face be convex. The occurrence of re-entering edges can and must be avoided by subdividing the corresponding face into several convex polygons. The coordinates of points on the solar paddles and the OPEP are given in a standard position relative to the box (solar array angle $\Phi = 0$ and OPEP angle $\Psi = 0$) together with the location of their axes. The program will then compute the rotation angle of the solar array and OPEP from their

attitude control logic and obtain the position of shadowing surfaces and experiments attached to paddles and OPEP.

The program operates by transforming the coordinates of the Sun and the Earth into the box coordinate system by means of a transformation matrix described in section IV-C.

Fewer points are involved in this transformation than in the reverse process. In this box coordinate system, the shadow cylinders of all the faces are then computed and the location of the experiments within or outside these cylinders is tested. If any experiment is found to be inside the shadow cylinder of any one surface, this experiment is in the shadow and no further testing is necessary for this experiment. Similarly, if the satellite is in the shadow of the earth, no shadow testing will be performed for any of the faces.

B. An Experiment Shadowed From the Sun by a Polygonal Plane Face.

1. The Equation of a Plane Formed by a Surface of the Main Box.

The vertices of the box are denoted by \bar{r}_i ($i = 1, 2, \dots, N$). Out of these N points various sets of k points ($k \geq 3$) are given as vertices of the corresponding faces. The first three points of each such set are used to determine the equation of the plane in which the face lies.

Care must be taken in the selection of these points, so that an accurate description of the surface is obtained from these points. In particular they must be chosen to lie on edges which are not too short

and not near parallel. This can always be achieved by arranging the points in proper order. If the first three points on the surface are denoted by \bar{r}_l , \bar{r}_m and \bar{r}_n the equation of the surface may be written in the form (see Appendix A).

$$\begin{vmatrix} x & y & z & 1 \\ x_l & y_l & z_l & 1 \\ x_m & y_m & z_m & 1 \\ x_n & y_n & z_n & 1 \end{vmatrix} = 0 \quad (1)$$

or alternately by:

$$A_i x + B_i y + C_i z + D_i = 0 \quad (2)$$

The four vector (A_i, B_i, C_i, D_i) is denoted by S_i and is taken as the analytic representation of the plane containing the i^{th} face. The vectors \bar{r} , \bar{r}_l , \bar{r}_m and \bar{r}_n are in a coordinate system which is fixed to the main box. If the three-vector (x_l, x_m, x_n) is denoted by \bar{X}_{lmn} with the corresponding notation for \bar{Y}_{lmn} and \bar{Z}_{lmn} and \bar{U} is defined as the vector $\bar{U} = (1, 1, 1)$ (see Appendix A); consequently.

$$\begin{aligned} A_i &= \bar{U} \cdot (\bar{Y}_{lmn} \times \bar{Z}_{lmn}) \\ B_i &= \bar{U} \cdot (\bar{Z}_{lmn} \times \bar{X}_{lmn}) \\ C_i &= \bar{U} \cdot (\bar{X}_{lmn} \times \bar{Y}_{lmn}) \\ D_i &= -\bar{X}_{lmn} \cdot (\bar{Y}_{lmn} \times \bar{Z}_{lmn}) \end{aligned} \quad (3)$$

2. The Equation of a Plane Formed by a Surface of the Solar Array.

\bar{r}_i and \bar{r}_i' represent position vectors of any solar array point in its zero and rotated position respectively. \bar{r}_{p0} represents the coordinates of any point on the axis of rotation. The axis of rotation is parallel to the x-axis, hence

$$\begin{aligned}x_i' &= x_i \\y_i' &= y_{p0} + (y_i - y_{p0}) \cos \Phi - (z_i - z_{p0}) \sin \Phi \\z_i' &= z_{p0} + (y_i - y_{p0}) \sin \Phi + (z_i - z_{p0}) \cos \Phi\end{aligned}\tag{4}$$

where Φ is the angle of rotation. (See Figure 3).

Introducing the Notation:

$\Delta x_i = x_i - x_{p0}$ with corresponding definitions for Δy_i , Δz_i , equation (4) can be rewritten:

$$\begin{aligned}x_i' &= x_i \\ \Delta y_i' &= \Delta y_i \cos \Phi - \Delta z_i \sin \Phi \\ \Delta z_i' &= \Delta y_i \sin \Phi + \Delta z_i \cos \Phi\end{aligned}\tag{5}$$

Equations (4) or (5) give the coordinates of any point attached to the paddle in its rotated position.

The rotated position coordinates of any three points on the surface can be used to obtain the vectors describing the planes containing the paddle faces. It is, however, more convenient to carry out the transformation directly on the vectors (A_i, B_i, C_i, D_i)

describing the plane, by equation (2). The 4-vector (A_i', B_i', C_i', D_i') describing the rotated plane is given in terms of $\bar{X}'_{lmn}, \bar{Y}'_{lmn}, \bar{Z}'_{lmn}$ by means of equation (3) where

$$\bar{X}'_{lmn} = x'_l, x'_m, x'_n$$

with corresponding definitions for \bar{Y}'_{lmn} and \bar{Z}'_{lmn} .

Further

$$\begin{aligned}\Delta\bar{X} &= \bar{X} - x_{po} \bar{U} \\ \Delta\bar{Y} &= \bar{Y} - y_{po} \bar{U} \\ \Delta\bar{Z} &= \bar{Z} - z_{po} \bar{U}\end{aligned}\tag{6}$$

where the subscripts l, m, n have been dropped for convenience. In terms of these quantities:

$$\begin{aligned}\bar{X}' &= \bar{X} \\ \bar{Y}' &= y_{po} \bar{U} + \Delta\bar{Y} \cos \Phi - \Delta\bar{Z} \sin \Phi \\ \bar{Z}' &= z_{po} \bar{U} + \Delta\bar{Y} \sin \Phi + \Delta\bar{Z} \cos \Phi\end{aligned}\tag{7}$$

Substitution of Equation (7) into (3) then results in the following equations:

$$\begin{aligned}A' &= A \\ B' &= B \cos \Phi - C \sin \Phi \\ C' &= B \sin \Phi + C \cos \Phi \\ D' &= D - B [y_{po} (\cos \Phi - 1) + z_{po} \sin \Phi] \\ &\quad + C [y_{po} \sin \Phi - z_{po} (\cos \Phi - 1)]\end{aligned}\tag{8}$$

3. OPEP Points.

The OPEP is assumed to be carrying only experiments, hence only the formulae concerning transformation of points are necessary. Further, the rotation takes place about an axis parallel to the z-axis. The formulae are consequently:

$$\begin{aligned}x_i' &= x_{T0} + (x_i - x_{T0}) \cos \Psi - (y_i - y_{T0}) \sin \Psi \\y_i' &= y_{T0} + (x_i - x_{T0}) \sin \Psi + (y_i - y_{T0}) \cos \Psi \\z_i' &= z_i\end{aligned}\tag{9}$$

where Ψ is the angle of rotation. (See Figure 4).

4. Sunny or Shady Side Test.

In terms of these vectors the sign of the product,

$$(\bar{S}_i \cdot \bar{R}_j)(\bar{S}_i \cdot \bar{R}_k) = s \text{ (See Appendix B)}\tag{10}$$

determines the position of points \bar{r}_j and \bar{r}_k relative to surface \bar{S}_i . In particular if $s < 0$, \bar{r}_j and \bar{r}_k lie on opposite sides of the surface, and if $s > 0$, \bar{r}_j and \bar{r}_k lie on the same side of the surface and for $s = 0$ at least one of the points lies on the surface. If now \bar{r}_j represents the Sun's coordinates and \bar{r}_k the coordinates of an experiment to be tested, $s \geq 0$ means then that the surface \bar{S}_i cannot cast a shadow on experiment \bar{r}_k . If, however, $s < 0$ further tests have to be performed to

determine whether the experiment lies inside or outside the shadow cylinder of the face.

For the box surface \bar{S}_i is defined by equation (3). For a solar array surface \bar{S}_i is defined by the 4-vector (A', B', C', D') which is given in equation (8).

If an experiment is attached to the main box its augmented position vector

$$\bar{R}_j = (x_j, y_j, z_j, 1) \quad (11)$$

may be substituted directly into equation (10) for the test. If the experiment is attached to the solar array

$$\bar{R}_j \equiv (x_j', y_j', z_j', 1) \quad (12)$$

where

$$x_j', y_j', z_j'$$

are given by equation (4). If an experiment is attached to the OPEP

$$\bar{R}_j \equiv (x_j', y_j', z_j', 1) \quad (13)$$

where

$$x_j', y_j', z_j'$$

are given by equation (9).

5. Shadow Cylinder Test

If $s < 0$ (where s is defined in equation (10) above) this establishes that the Sun and the experiment lie on opposite sides of the surface. Further tests have to be performed to determine whether the experiment lies inside or outside the shadow cylinder of the face.

This testing is accomplished by projecting both face and experiment onto a plane perpendicular to the Sun's radius vector. A polygonal face will always be projected into a polygon, unless the Sun's radius vector is parallel to the face, in which case no further testing need be performed for this combination of surface and experiment. Let the first vertex \bar{r}_1 (chosen arbitrarily from among the M vertices on the face) and the other vertices $\bar{r}_p, \bar{r}_q \dots$ etc. (taken in order around the face) be renamed \bar{r}_i ($i = 0 \dots M-1$).

If \bar{r}_0 is now chosen as origin, the coordinates of the vertices relative to this origin are given by:

$$\bar{r}_i' = \bar{r}_i - \bar{r}_0 \quad (14)$$

in particular

$$\bar{r}_0' = (0, 0, 0)$$

Further

$$\bar{r}_{sv}' = \bar{r}_{sv} - \bar{r}_0 \quad (15)$$

where \bar{r}_{sv} is the vector from satellite to Sun. (Note: because of the relative size of the components of \bar{r}_{sv} and \bar{r}_o the vectors \bar{r}'_{sv} and \bar{r}_{sv} will in general be numerically identical).

In terms of these vectors, a coordinate system is now set up in the test plane (i.e. the plane perpendicular to \bar{r}'_{sv} by means of the unit vectors \bar{i}'' , \bar{j}'' .

$$\begin{aligned}\bar{i}'' &= \frac{\bar{r}'_{sv} \times \bar{r}_1'}{|\bar{r}'_{sv} \times \bar{r}_1'|} \\ \bar{j}'' &= \frac{\bar{r}'_{sv} \times \bar{i}''}{|\bar{r}'_{sv}|}\end{aligned}\tag{16}$$

The coordinates of the projections of the vertices onto the test plane are now given by:

$$p_i'' = x_i'' \bar{i}'' + y_i'' \bar{j}''\tag{17}$$

where

$$\begin{aligned}x_i'' &= \bar{r}_j' \cdot \bar{i}'' \\ y_i'' &= \bar{r}_i' \cdot \bar{j}''\end{aligned}\tag{i = 0 \cdots M-1}$$

and the coordinates of the projection of the experiment (n) are given by;

$$\begin{aligned}\bar{q}_n'' &= x_n'' \bar{i}'' + y_n'' \bar{j}'' \\ x_n'' &= \bar{r}_n' \cdot \bar{i}'' \\ y_n'' &= \bar{r}_n' \cdot \bar{j}''\end{aligned}\tag{18}$$

In this test plane, the shadow cylinder is represented by a polygon with the M sides

$$\bar{L}_{j,j+1} \quad (j = 0 \cdots M-1)$$

where $L_{j,j+1}$ is the straight line containing the projection of the vertices \bar{r}_j' and \bar{r}_{j+1}' (Note: In this connection it is convenient to equate \bar{r}_m' to \bar{r}_0'). The equation of the side $\bar{L}_{j,j+1}$ is given by (See Appendix C):

$$\begin{vmatrix} x'' & y'' & 1 \\ x_j'' & y_j'' & 1 \\ x_{j+1}'' & y_{j+1}'' & 1 \end{vmatrix} = 0\tag{19}$$

or alternately:

$$a_j x'' + b_j y'' + c_j = 0\tag{20}$$

where

$$\begin{aligned} a_j &= y_j'' - y_{j+1}'' \\ b_j &= -x_j'' + x_{j+1}'' \\ c_j &= x_j'' y_{j+1}'' - x_{j+1}'' y_j'' \end{aligned} \quad (21)$$

The vector (a_j, b_j, c_j) is taken to represent the line $\bar{L}_{j,j+1}$ and the three vector $\bar{Q}_n = (x_n'', y_n'', 1)$ represents the point \bar{q}_n'' ; and let

$$\bar{P}_{j+2} = (x_{j+2}'', y_{j+2}'', 1)$$

represent the $j + 2$ vertex of polygon projected onto the test plane. In terms of these vectors, the experiment represented by the vector \bar{Q}_n lies inside the polygon in the test plane (and consequently inside the shadow cylinder of the face) if:

$$u = (\bar{Q}_n \cdot \bar{L}_{j,j+1})(\bar{P}_{j+2} \cdot \bar{L}_{j,j+1}) > 0 \quad (22)$$

for all j between 0 and $M-1$. See Appendix D for the mathematical derivation of this expression.

C. Ideal Control Laws and Definition of Axes Systems

The geometry of the OGO satellite is described in a coordinate system attached to the main structure, (box coordinates), whereas the orbit and consequently the vectors from the Sun and Earth to the satellite as well as the velocity of the satellite are given in a different

coordinate system. In order to carry out the test described in section IVB, the components of all vectors have to be known in a single coordinate system. It is convenient to use the box coordinate system to carry out this testing, since fewer transformations have to be made.

In order to relate these coordinate systems and to establish the transformation matrices, the ideal control laws for the OGO satellite were assumed. Further, these relations are written entirely in terms of the vectors \bar{r}_{VE} , $\dot{\bar{r}}_{VE}$ and \bar{r}_{SV} . Consequently, the transformations will be valid, no matter what coordinate system is used in describing the orbit.

In order to describe the transformation from the orbital to the box coordinate system, a matrix is established. In addition, an angle of rotation must be determined for the solar array and another for the OPEP.

In the following, four coordinate systems are considered. Each coordinate system is defined by a triple $(\bar{i}, \bar{j}, \bar{k})$ of mutually orthogonal unit vectors. The systems attached to box, solar array and OPEP are identified by subscripts B, p and T respectively. Quantities without subscripts refer to the orbital coordinate system.

The three vectors \bar{r}_{VE} , $\dot{\bar{r}}_{VE}$, \bar{r}_{SV} (the position and velocity vector of the satellite with respect to the Earth and the position of the Sun with respect to the satellite) are given in the orbital coordinate system.

1. The Orbital To Box Transformation Matrix.

The ideal control laws are specified in Reference 5.

- a). The positive z_B face is aligned with the radius vector from the center of the Earth to the satellite.
- b). The solar array is normal to incident sunlight.
- c). The Sun does not shine on the positive y_B face. (Reference 5).
- d). The positive x face of the OPEP faces forward in the plane of the orbit. (Reference 6). These laws lead to the following equations:

Due to a).

$$\bar{k}_B = - \frac{\bar{r}_{VE}}{|\bar{r}_{VE}|} \quad (23)$$

Due to b).

$$\bar{j}_P = \frac{\bar{r}_{SV}}{|\bar{r}_{SV}|} \quad (24)$$

Since the paddle rotates about an axis parallel to i_B

$$\bar{j}_P = \bar{j}_B \cos \Phi + \bar{k}_B \sin \Phi \quad (25)$$

From (equation 25)

$$\bar{j}_P \cdot \bar{i}_B = 0$$

and by definition

$$\bar{k}_B \cdot \bar{i}_B = 0$$

Consequently

$$\bar{i}_B = \pm \frac{\bar{k}_B \times \bar{j}_P}{|\bar{k}_B \times \bar{j}_P|} \quad (26)$$

The vector triple is completed by defining

$$\bar{j}_B = \bar{k}_B \times \bar{i}_B \quad (27)$$

According to c).

$$\bar{j}_B \cdot \bar{r}_{SV} < 0 \quad (28)$$

Equation (28) resolves the ambiguity in equation (26) as follows: Substituting from (26) into (27):

$$\bar{j}_B = \pm \frac{\bar{k}_B \times (\bar{k}_B \times \bar{j}_P)}{|\bar{k}_B \times \bar{j}_P|} = \pm \frac{[(\bar{k}_B \cdot \bar{j}_P) \bar{k}_B - (\bar{k}_B \cdot \bar{k}_B) \bar{j}_P]}{|\bar{k}_B \times \bar{j}_P|} \quad (29)$$

From (24)

$$\bar{r}_{SV} = \bar{j}_P |\bar{r}_{SV}| \quad (30)$$

From equations (28), (29) and (30)

$$0 > \bar{\mathbf{j}}_{\mathbf{B}} \cdot \bar{\mathbf{r}}_{\mathbf{SV}} = \pm |\bar{\mathbf{r}}_{\mathbf{SV}}| \left[(\bar{\mathbf{k}}_{\mathbf{B}} \cdot \bar{\mathbf{j}}_{\mathbf{P}})^2 - \bar{\mathbf{k}}_{\mathbf{B}}^2 \bar{\mathbf{j}}_{\mathbf{P}}^2 \right] \quad (31)$$

From (25) $\bar{\mathbf{k}}_{\mathbf{B}} \cdot \bar{\mathbf{j}}_{\mathbf{P}} = \sin \Phi$

$$0 > \bar{\mathbf{j}}_{\mathbf{B}} \cdot \bar{\mathbf{r}}_{\mathbf{SV}} = \pm |\bar{\mathbf{r}}_{\mathbf{SV}}| [\sin^2 \Phi - 1] \quad (32)$$

In Equation (32) the term $|\bar{\mathbf{r}}_{\mathbf{SV}}| [\sin^2 \Phi - 1]$ is less than or equal to zero, it follows that the plus sign must be chosen in equations (26) and (29).

If now $\bar{\mathbf{r}}$ is an arbitrary vector with components x, y, z in the orbit system and coordinates $x_{\mathbf{B}}, y_{\mathbf{B}}, z_{\mathbf{B}}$ in the box system

$$x_{\mathbf{B}} = \bar{\mathbf{r}} \cdot \bar{\mathbf{i}}_{\mathbf{B}} \quad y_{\mathbf{B}} = \bar{\mathbf{r}} \cdot \bar{\mathbf{j}}_{\mathbf{B}} \quad z_{\mathbf{B}} = \bar{\mathbf{r}} \cdot \bar{\mathbf{k}}_{\mathbf{B}} \quad (33)$$

or in matrix notation

$$\begin{bmatrix} x_{\mathbf{B}} \\ y_{\mathbf{B}} \\ z_{\mathbf{B}} \end{bmatrix} = \begin{bmatrix} \bar{\mathbf{i}}_{\mathbf{B}} \cdot \bar{\mathbf{i}} & \bar{\mathbf{i}}_{\mathbf{B}} \cdot \bar{\mathbf{j}} & \bar{\mathbf{i}}_{\mathbf{B}} \cdot \bar{\mathbf{k}} \\ \bar{\mathbf{j}}_{\mathbf{B}} \cdot \bar{\mathbf{i}} & \bar{\mathbf{j}}_{\mathbf{B}} \cdot \bar{\mathbf{j}} & \bar{\mathbf{j}}_{\mathbf{B}} \cdot \bar{\mathbf{k}} \\ \bar{\mathbf{k}}_{\mathbf{B}} \cdot \bar{\mathbf{i}} & \bar{\mathbf{k}}_{\mathbf{B}} \cdot \bar{\mathbf{j}} & \bar{\mathbf{k}}_{\mathbf{B}} \cdot \bar{\mathbf{k}} \end{bmatrix} \begin{bmatrix} x \\ y \\ z \end{bmatrix} \quad (34)$$

The vectors $\bar{\mathbf{i}}_{\mathbf{B}}, \bar{\mathbf{j}}_{\mathbf{B}}, \bar{\mathbf{k}}_{\mathbf{B}}$ are defined by equations (23), (26) and (27).

2. The Solar Array Angle Φ .

The solar array angle Φ is obtained from equations (24) and (25).

$$\begin{aligned}\frac{\bar{r}_{sv}}{|\bar{r}_{sv}|} \cdot \bar{j}_B &= \cos \Phi \\ \frac{\bar{r}_{sv}}{|\bar{r}_{sv}|} \cdot \bar{k}_B &= \sin \Phi\end{aligned}\tag{35}$$

For the transformations, only $\cos \Phi$ and $\sin \Phi$ are needed, the angle Φ need not be computed.

3. The OPEP Angle Ψ .

The vector \bar{i}_T is in the plane of the orbit and

$$\bar{k}_T = \bar{k}_B\tag{36}$$

The orbit plane is defined by the angular momentum vector \bar{H}

$$\bar{H} = \bar{r}_{VE} \times \dot{\bar{r}}_{VE}\tag{37}$$

\bar{H} is normal to the orbit plane hence

$$\bar{i}_T = \pm \frac{\bar{k}_T \times \bar{H}}{|\bar{k}_T \times \bar{H}|}\tag{38}$$

Further, \bar{i}_T points in the direction of motion, i.e;

$$\bar{i}_T \cdot \dot{\bar{r}}_{VE} > 0\tag{39}$$

Substituting (23) and (37) into (38) yields:

$$\begin{aligned}\bar{\mathbf{i}}_T &= \pm \frac{(-\bar{\mathbf{r}}_{VE}) \times (\bar{\mathbf{r}}_{VE} \times \dot{\bar{\mathbf{r}}}_{VE})}{|\bar{\mathbf{r}}_{VE}| |\bar{\mathbf{k}}_T \times \bar{\mathbf{H}}|} \\ &= \pm \frac{1}{|\bar{\mathbf{r}}_{VE}| |\bar{\mathbf{k}}_T \times \bar{\mathbf{H}}|} \left[(\bar{\mathbf{r}}_{VE} \cdot \bar{\mathbf{r}}_{VE}) \dot{\bar{\mathbf{r}}}_{VE} - (\bar{\mathbf{r}}_{VE} \cdot \dot{\bar{\mathbf{r}}}_{VE}) \bar{\mathbf{r}}_{VE} \right]\end{aligned}\quad (40)$$

Substituting (40) into (39):

$$0 < \bar{\mathbf{i}}_T \cdot \dot{\bar{\mathbf{r}}}_{VE} = \pm \frac{1}{|\bar{\mathbf{r}}_{VE}| |\bar{\mathbf{k}}_T \times \bar{\mathbf{H}}|} \left[|\bar{\mathbf{r}}_{VE}|^2 |\dot{\bar{\mathbf{r}}}_{VE}|^2 - (\bar{\mathbf{r}}_{VE} \cdot \dot{\bar{\mathbf{r}}}_{VE})^2 \right]$$

by Schwartz's inequality the expression in braces is positive, hence the plus sign has to be selected in equation (38).

The vector triple is now completed by:

$$\bar{\mathbf{j}}_T = \bar{\mathbf{k}}_T \times \bar{\mathbf{i}}_T \quad (41)$$

The OPEP angle Ψ is now obtained from the equations:

$$\begin{aligned}\bar{\mathbf{i}}_T \cdot \bar{\mathbf{i}}_B &= \cos \Psi \\ \bar{\mathbf{i}}_T \cdot \bar{\mathbf{j}}_B &= \sin \Psi\end{aligned}\quad (42)$$

Again, for the transformations, only $\cos \Psi$ and $\sin \Psi$ are needed.

D. Detailed Shadow Testing Procedure.

The equations of the planes containing the potential shadowing faces are established initially and the corresponding vectors (A_i ,

B_i, C_i, D_i). As described in equations (1) and (2) are computed and stored, together with the list of its vertices. This is done initially for both box and solar array faces. The solar array faces, however, must be rotated at every test time after the angle Φ has been established according to equation (8). The testing at every point is now carried out in the following sequence:

1. Satellite Earth Shadow Testing.

It is determined whether the satellite is in the Earth's shadow cone. If it is, the possible shadowing effect of satellite components need, of course, not be determined. If this test, however, shows the satellite to be in the sunlight, testing has to be carried out for each individual experiment as follows:

2. Individual Experiment Testing.

- a). The matrix described in equation (34) is computed.
- b). The solar array angle Φ is computed by equations (35).
- c). The OPEP angle Ψ is computed by equations (42).
- d). The coordinates of Sun and Earth with respect to the box are transformed from the orbital to the box coordinate system by equation (34).
- e). The coordinates of the experiment are transformed, if necessary, (i.e. if the experiment moves with either the solar array or the OPEP) by equations (4) or (9) respectively.

Items a) through d) of this list to be performed only once for each set of tests (i.e. for each time point). Item e) has to be performed for each experiment.

After all this setup work has been completed, the shadow tests are carried out for this particular experiment designated by (n) as follows:

All the faces are tested in turn until:

a. Either all surfaces have been tested and it has been established that none casts a shadow on experiment (n) . In this case, experiment (n) has been established to receive incident sunlight and the next experiment $(n+1)$ is tested.

b. Or a face has been found which casts a shadow on experiment (n) . In this case, experiment (n) has been established not to receive incident sunlight, the effect of the remaining faces need not be examined, and the next experiment $(n+1)$ is then tested.

The hierarchy of tests, for a particular experiment (n) and face (i) is described in the following:

1. Test whether face (i) is connected to solar array, and carry out, if necessary, the transformation described in equations (8).

2. Test whether the experiment lies on the sunny side or the shady side of the plane containing face (i) by using the augmented box coordinates of the Sun as \bar{R}_j and the augmented box coordinates of the experiment as \bar{R}_k and substituting in equation (10).

If $s > 0$ the experiment is on the sunny side, this face cannot cast a shadow on experiment (n) and the next face is then tested.

If $s = 0$ either the Sun, or the experiment, or both lie on the surface and the surface is assumed not to cast a shadow on experiment (n). In this case, the next face is tested.

If $s < 0$ the experiment (n) lies on the shady side of face \bar{S}_i . See Appendix B for more details. If it also lies within the shadow cylinder of the face it will be in shadow.

3. Test whether experiment (n) is within the shadow cylinder of the face (i). In order to carry out this test, the following steps have to be taken:

- a). Compute the vectors \bar{r}_i' , \bar{r}_o' and \bar{r}_{sv}' for the experiment (n), all the vertices of faces (i) and the Sun by equations (14) and (15).
- b). Set up the coordinate system (i'' , j'') in the test plane by equation (16).
- c). Compute the coordinates (x'' , y'') of the vertices and the experiment in the test plane (i.e. the plane normal to the Sun's radius vector), by equations (17) and (18).
- d). Compute u by equation (22) for edge (j).

If $u < 0$, the experiment lies outside the shadow cylinder of this face, this face does not shadow experiment (n) and the next face $i + 1$ is then tested.

If $u = 0$ the experiment is also taken to be outside the shadow cylinder and the next face $(i + 1)$ is then tested.

If $u > 0$ for the j^{th} edge the next edge $(j + 1)$ of the face is tested until one edge has been found for which $u < 0$. Then this face (i) does not cast a shadow and the next face $(i + 1)$ is tested. If all edges of a face have been tested and $u > 0$ for all edges then this face (i) casts a shadow on experiment (n). The program then proceeds to the next experiment $(n + 1)$. This is explained in more detail in Appendix D.

V. MATHEMATICAL MODEL FOR HEAT INPUTS TO AN ARBITRARILY ORIENTED SURFACE OF OGO.

A. Direct Solar Radiant Heat.

This is the heat flux $\dot{q}_{ns}(t)$ incident upon a surface of the n th experiment at time t , which radiates directly from the Sun. It is given by:

$$\dot{q}_{ns}(t) = I(t) \sigma f(i_n(t)) \left[|\bar{r}_{sv}(t)| \right]^{-2} \quad (43)$$

here: $I(t) = 0$ or 1 depending on whether the experiment is in shadow or Sun, σ is the incident radiation on a unit area at a distance of 1 AU from the Sun, and i_n the angle of incidence given by

$$\cos i_n = \bar{n}_n \cdot \frac{\bar{r}_{sv}}{|\bar{r}_{sv}|} \quad (44)$$

where \bar{n}_n is the normal to the experiment surface in box coordinates.

If $\cos i_n < 0$, the experiment surface faces away from the Sun and receives no radiation. This is expressed formally by

$$f(i_n) = \frac{1}{2} (\cos i_n + |\cos i_n|) \quad (45)$$

In the case of an earth satellite the variation of $|\bar{r}_{sv}|$ is too small to matter and a constant value may be used. The accumulated radiation

between times t_o and $(t_o + N\Delta t)$ is given by:

$$q_{ns}(t_o, t_o + N\Delta t) = \sum_{k=0}^{N-1} \frac{1}{2} [\dot{q}_{ns}(t_o + k\Delta t) + \dot{q}_{ns}(t_o + (k+1)\Delta t)] A_n \Delta t_k \quad (46)$$

where

A_n = the area of experiment (n) .

B. Reflected Solar Radiant Heat.

This is the heat flux $\dot{q}_{na}(t)$, incident upon a surface of the nth experiment at time t , which originates at the Sun and reflects from the Earth. In integral form (See Figure 5).

$$\dot{q}_{na}(t) = a \sigma \int f_a(\gamma_1, \gamma_2, \gamma_3, r) dA \quad (47)$$

where,

a = the albedo = the fraction of the solar constant σ which is reflected away from the Earth. The value for a is about 0.34 (Reference 7).

$\sigma = 1.97 \pm 0.01 \text{ cal cm}^{-2} \text{ minutes}^{-1} = 0.1374 \text{ watts cm}^{-2} = \text{flux}$
of total radiation received outside the Earth's atmosphere
per unit area at mean Sun-Earth distance (Reference 7).

$$f_a(\gamma_1, \gamma_2, \gamma_3, r) = \left(\frac{\cos \gamma_1 \cos \gamma_2 \cos \gamma_3}{\pi r^2} \right) \begin{matrix} \text{if } \cos \gamma_1 > 0 \text{ and} \\ \cos \gamma_2 > 0 \text{ and } \cos \gamma_3 > 0 \end{matrix}$$

$$f_a = 0 \text{ if } \cos \gamma_1 \leq 0 \text{ or } \cos \gamma_2 \leq 0 \text{ or } \cos \gamma_3 \leq 0$$

dA = an elemental area of the Earth's surface (Figure 5).

γ_1 = the angle of incidence of the Sun's rays on the Earth's surface element (Figure 5).

γ_2 = the angle between the radius vector \bar{r} which points from dA to the vehicle and the normal to the Earth's surface element dA (Figure 5).

γ_3 = the angle between the vector \bar{r} and the unit outward normal to the experiment surface (Figure 5).

\bar{r} = the vector which points from the vehicle to dA (Figure 5).

The method of numerically evaluating Equation (47) is given in the following paragraphs.

Let θ be the angle between \bar{r}_{VE} and the radius vector from the center of the Earth to the surface element in question, and α be the angle corresponding to the longitude in the plane normal to \bar{r}_{VE} the zero line being the projection of \bar{i}_B on this plane. (See Figure 5).

The part of the sphere which the satellite can see is then characterized by

$$0 \leq \alpha \leq 2\pi$$

$$0 \leq \theta \leq \beta$$

where

$$\cos \beta = \frac{a_E}{|\bar{\mathbf{r}}_{VE}|} \quad (48)$$

here a_E is the radius of the Earth. The range of θ and α is now subdivided such that

$$\Delta\theta = \beta/L$$

$$\Delta\alpha = 2\pi/M$$

The normal to the Earth's surface element ΔA_{lm} is approximated by

$$\bar{\mathbf{N}}_{lm} = \bar{\mathbf{i}}_B \sin \theta_l \cos \alpha_m - \bar{\mathbf{j}}_B \sin \theta_l \sin \alpha_m - \bar{\mathbf{k}}_B \cos \theta_l \quad (49)$$

where

$$\begin{aligned} \theta_l &= \frac{\left(l + \frac{1}{2}\right)\beta}{L}, \quad l = 0, 1, 2, 3 \dots, L-1 \\ \alpha_m &= \frac{2\pi \left(m + \frac{1}{2}\right)}{M}, \quad m = 0, 1, 2, 3 \dots, M-1 \end{aligned} \quad (50)$$

The position vector of this surface element from the satellite is given by:

$$\bar{\mathbf{r}}_{lm} = \bar{\mathbf{r}}_{VE} + a_E \bar{\mathbf{N}}_{lm} \quad (51)$$

Note that the \bar{r}_{vE} vector in this equation is given in the box coordinate system.

It may now be determined whether radiation from this segment of the Earth's surface reaches experiment (n) by using vector \bar{r}_{lm} in place of the Sun vector \bar{r}_{sv} in the tests described in section IV. Note in particular that the only additional set up work which has to be done is the transformation of the experiment into box coordinates (item e when necessary) and only the tests have to be performed.

The cosines of three angles determine the amount of incident radiation received from the lit surface of the earth. They are:

- a). The angle of incidence γ_1 of the Sun's rays on the surface element. This cosine determines the intensity of the illumination of the surface element and is given by the equation,

$$\cos \gamma_{1lm} = \bar{N}_{lm} \cdot \frac{\bar{r}_{slm}}{|\bar{r}_{slm}|} \quad (52)$$

where

$$\bar{r}_{slm} = \bar{r}_{se} - a_E \bar{N}_{lm}$$

The degree of accuracy required for this computation allows

$\bar{r}_{slm} = \bar{r}_{se}$ and equation (52) then becomes:

$$\cos \gamma_{1lm} = \bar{N}_{lm} \cdot \frac{\bar{r}_{se}}{|\bar{r}_{se}|} \quad (53)$$

b). The angle γ_{2lm} between the radius vector from the surface element to the vehicle and the normal to the surface element. This angle controls the size of the surface element as seen from the satellite. The cosine of this angle is given by equation (54).

$$\cos \gamma_{2lm} = - \frac{\bar{r}_{lm}}{|\bar{r}_{lm}|} \cdot \bar{N}_{lm} \quad (54)$$

\bar{r}_{lm} in this equation is defined by equation (51);

c). Finally the angle γ_{3lm} between the incident radiation and the normal to the experiment surface determines the solid angle subtended by the experiment at the origin of radiation. This angle γ_{3lm} is given by equation (55)

$$\cos \gamma_{3lm} = \bar{n}_n \cdot \frac{\bar{r}_{lm}}{|\bar{r}_{lm}|} \quad (55)$$

\bar{n}_n here is the normal to the experiment surface in box coordinates.

1. Contribution due to a lit surface element:

The contribution of the particular element ΔA_{lm} to the reflected solar heat flux at time t is given by equation (56).

$$\Delta \dot{q}_{na}(t) = \frac{a\sigma I_{lm} f(\gamma_{1lm}) f(\gamma_{2lm}) (f_{3lm}) \Delta A_{lm}}{\pi |\bar{r}_{lm}|^2} \quad (56)$$

$$I_{lm} = \begin{cases} 0 & \text{if the experiment is shaded by the satellite} \\ 1 & \text{if the experiment is not shaded} \end{cases}$$

Here

$$f(\gamma) = \frac{1}{2} (\cos \gamma + |\cos \gamma|)$$

and

$$\Delta A_{lm} = a_E^2 \Delta \theta \Delta \alpha \sin \theta_l \quad (57)$$

In equation (56) γ_{1lm} , γ_{2lm} , γ_{3lm} and r_{lm} are functions of time. The total reflected solar heat flux received from all surface elements is

$$\dot{q}_{na}(t) = \sum_{l,m} \Delta \dot{q}_{na}(t) \quad (58)$$

This may be accumulated over a time interval from t_o to $(t_o + N\Delta t)$

$$q_{na}(t_o, t_o + N\Delta t) = \sum_{k=0}^{N-1} \frac{1}{2} [\dot{q}_{na}(t_o + k\Delta t) + \dot{q}_{na}(t_o + (k+1)\Delta t)] A_n \Delta t_k \quad (59)$$

C. Earth Emitted Radiant Heat

This is the heat flux $\dot{q}_{nE}(t)$ incident upon a surface of the n th experiment at time t , which is emitted by the Earth. In integral form (See Figure 5).

$$\dot{q}_{nE}(t) = \Lambda \int f_E(\gamma_2, \gamma_3, r) dA \quad (60)$$

where

$\Lambda = 0.02215 \text{ watts cm}^{-2}$ = the emittance per unit area of the surface of the Earth.

$$f_E = \frac{\cos \gamma_2 \cos \gamma_3}{\pi r^2} \quad \text{if } \cos \gamma_2 > 0 \text{ and } \cos \gamma_3 > 0$$

$$= 0 \quad \text{if } \cos \gamma_2 \leq 0 \text{ or } \cos \gamma_3 \leq 0 .$$

This is evaluated numerically and is analogous to (56), (58), and (59), except that the angle of incidence of solar energy is immaterial.

The equations are as follows:

The contribution from the element ΔA_{lm} to the Earth emitted heat flux at time t is given by equation (61).

$$\Delta \dot{q}_{nE}(t) = \frac{\Lambda I_{lm} f(\gamma_{2lm}) f(\gamma_{3lm}) \Delta A_{lm}}{\pi r_{lm}^2} \quad (61)$$

The total Earth emitted heat flux received from all surface elements is

$$\dot{q}_{nE}(t) = \sum_{l,m} \Delta \dot{q}_{nE}(t) \quad (62)$$

The accumulation over a time interval from t_o to $(t_o + N\Delta t)$ is

$$q_{nE}(t_o, t_o + N\Delta t) = \sum_{k=0}^{N-1} \frac{1}{2} \left[\dot{q}_{nE}(t_o + k\Delta t) + \dot{q}_{nE}(t_o + (k+1)\Delta t) \right] A_n \Delta t_k \quad (63)$$

VI. RESULTS AND DISCUSSION

A. Shadow Study

Figures 6 through 8 present the amount of time per orbit that the EGO S-49 experiments spend in the shadow of the earth, the main satellite structure (the box) or of the solar array. These data are for three faces of the main box $+z_B$, $-z_B$ and $-y_B$ for the boom or appendage mounted experiments (E. P. 1 through E. P. 6), and for the orbital plane experiment package (OPEP 1 and 2). The coordinates for the sides of the main box and the experiments are shown in Section III of this document. In the case of the shadowing of the faces of main box test points were assumed to be along the axes of the box coordinate system and slightly above the surface (0.1 inch). The shadow history of the test point of each face is assumed to closely approximate the shadow history of the face itself. The test point device was incorporated to facilitate the mathematical description and programming of the system. The coordinates of the main box test points and normals are as follows:

Coordinates

Box Experiment	x (inches)	y (inches)	z (inches)
+x	14.707	0	0
-x	-14.707	0	0
+y	0	23.6	0
-y	0	-43.6	0
+z	0	0	15.083
-z	0	0	-15.083
Normals			
+x	1.0	0	0
-x	-1.0	0	0
+y	0	1.0	0
-y	0	-1.0	0
+z	0	0	1.0
-z	0	0	-1.0

The study for shadowing is based on a nominal orbit (See Section III for injection conditions) with a launch date of May 15, 1964 at 13.0 hours U. T.

1. The Main Box Experiments

Figure 6 shows the history of shadow time per orbit for a year of flight time for the $+z_B$, $-z_B$ and $-y_B$ faces of the main box. The figure indicates that for the $+z_B$ and $-z_B$ faces the shadow time per orbit varies between approximately 1 hour and 41.0 hours. The $-y_B$ face experiment, however, spends practically all of its time in sunlight. During the first 34 days in orbit the $-y_B$ face experiences shadows of about 0.5 hours after which time it senses full sunlight except between the 144th and 152nd days after launch when the shadow time gets only as high as 2.5 hours. At about the 265th day after launch, the $-y_B$ face again goes into a period during which it senses about 0.5 hours shadow per orbit. The shadow history of this face (in fact of the whole satellite and experiments) is a function of the time of launch. Consequently, for other launch dates the shadow history will be different.

2. Boom Mounted Experiments

The time-in-shadow history of the boom mounted experiments (E. P. 1 through E. P. 6) is shown in Figure 7. This time history curve is typical of any launch date, however the curve set would be different for different launch dates.

The figure clearly shows that the experiments in the order E. P. 1, E. P. 2, E. P. 3, E. P. 5, E. P. 6 (E. P. 4 = E. P. 6) are exposed to increasingly more sunlight. The maximum shadow time per orbit

varies from almost 40 hours for E. P. 1 to about 2.5 hours for E. P. 4 and 6.

3. OPEP

Figure 8 presents the time-in-shadow histories of the orbit plane experiment packages (OPEP). The experiment packages, OPEP 1 and OPEP 2 experience some shadow time during every orbit. These shadow times, however, vary from 41.0 hours per orbit to less than 1.0 hours per orbit. Again, as in the other cases, this curve set will be different for different launch dates.

B. Heat Inputs

Figures 9 through 20 present the heat inputs incident upon the different faces of the satellite as a function of time from perigee for the first orbital period (42.75 hours). These heat inputs include the Earth emitted heat flux \dot{q}_E , the direct solar heat flux \dot{q}_s and the solar reflected heat flux \dot{q}_a . The solar heat input to an experiment is set to zero if that particular experiment is shielded from the Sun by the Earth, the main box or the solar array. If an experiment is in the eclipse of the Earth the reflected solar (as well as the direct solar) heat input is set equal to zero. However, the effects of shadowing of an experiment from the Earth by the main box or the solar array is not considered in the computation of the solar reflected or Earth emitted heat inputs to that particular experiment. The reflected solar heat

flux is calculated by two different methods. The exact value is computed by numerically evaluating the integral given by equation (47). The method of calculating the approximate values is given in Reference 8. In this method an average value is assumed for γ_1 in equation (47). It is assumed that γ_1 (average) is the angle between the vector from the Earth to the Sun and the vector from the Earth to the satellite. In other words for a given location of the Earth, Sun and vehicle, the approximate reflected solar heat input depends only upon the angle between the experiment's normal and the Earth vehicle vector. The Earth emitted and solar reflected heat inputs are negligibly small when the satellite is beyond an altitude of 20,000 nautical miles or correspondingly 2.63 hours of flight time from perigee. The data in these figures are based on a time of injection into orbit of May 15, 1964 at 8.0 hours U. T. These curves are intended to demonstrate the capability to calculate heat inputs rather than to provide design data. The values of the Earth emitted heat inputs depend only upon the shape of the orbit and are independent of launch time. The direct solar and reflected solar heat inputs depend upon the relative locations of the Earth, the Sun and the vehicle; consequently they are dependent upon the launch time. The unit normals to the various S-49 experiments are given in section III.

1. The Main Box

a. Earth Emitted Heat Inputs

Figure 9 presents the Earth emitted heat inputs \dot{q}_E to the main box as a function of time from perigee. The $+z_b$ face has the largest Earth emitted heat input since it always faces the Earth. Conversely, the $-z_b$ face has a zero Earth emitted heat input. The $+x_B$, $-x_B$, $+y_B$, and the $-y_b$ faces all have equal Earth emitted heat inputs due to geometrical symmetry with respect to the Earth.

b. Direct Solar Heat Inputs.

Figure 10 presents the direct solar heat inputs (\dot{q}_s) to the main box as a function of time from perigee. This is a typical curve. The solar heat inputs to the $+x_B$, $-x_B$ and $+y_B$ face are always zero. This is true since the OGO satellite is controlled such that these faces receive no direct solar heat.

c. Reflected Solar Heat Inputs.

Figure 11 presents a comparison between the exact and approximate values of the reflected solar heat inputs. The $+z_B$ face has the largest reflected solar heat input since it faces the Earth. The $-z_B$ face has zero reflected solar heat inputs since it faces away from the Earth. The exact value of the reflected solar heat inputs to the $+x_B$ and $-x_B$ faces are equal since there is symmetry with respect to these faces and the sun-lit portion of the Earth. The approximate values of

the reflected solar heat inputs to the $+x_B$, $-x_B$, $+y_B$ and $-y_B$ faces are all equal. This is true since an average value is assumed for γ_1 in equation 47. It is assumed that γ_1 (average) is the angle between the vector from the Earth to the Sun and the vector from the Earth to the satellite. This is tantamount to assuming that for a given Earth, Sun and satellite configuration the amount of reflected solar heat inputs depends only upon the angle between the normal to the surface and the Earth-satellite line. Figure 11 shows that the largest difference between the exact and approximate value is 1.16 milliwatts/cm².

2. Boom Mounted Experiments

Figures 12 through 14 present the heat inputs to the boom mounted experiment packages (E. P. 1, E. P. 2, E. P. 3, E. P. 4, E. P. 5, and E. P. 6) as a function of time from perigee. The normals which define the orientation of the faces which have the various heats incident upon them are given in Section III of this report. These particular faces were chosen for investigation since they have the largest openings through which radiant heat may enter to the experiment packages.

a. Earth Emitted Heat.

Figure 12 shows the Earth emitted heat inputs to the experiment packages. All six experiment packages have equal Earth emitted heat input time histories. This is true since the normals to these experiments are parallel to the surface of the Earth.

b. Direct Solar Heat Inputs.

Figure 13 shows the direct solar heat inputs to the experiment packages. E. P. 4 and E. P. 6 have the same value of solar heat inputs since their normals point in the same direction. The direct solar heat inputs to E. P. 1, E. P. 2, E. P. 3 and E. P. 5 are identically zero. This is true since the normals to these experiments are oriented such that they never receive sunlight.

c. Reflected Solar Heat Inputs.

Figure 14 presents a comparison between the exact and approximate values of the reflected solar heat inputs to the boom mounted experiment packages. E. P. 4 and E. P. 6 have equal exact reflected solar heat flux since their normals are equal. Likewise E. P. 2, E. P. 3, and E. P. 5 have equal exact reflected solar heat flux because their normals are equal. E. P. 1 through E. P. 6 have equal values of approximate reflected solar heat flux since the angles between their normals and the Earth vehicle vector are all equal, i. e. ,

$$\cos^{-1} \left(\frac{\bar{r}_{VE}}{|\bar{r}_{VE}|} \cdot \bar{n} \right) = 90^\circ$$

Figure 14 shows that the largest difference between the exact and approximate values is 1.36 millwatts/cm².

2. The Solar Oriented Experiment Packages

The solar oriented experiment packages (SOEP 1 and SOEP 2) both have their normals pointing toward the Sun and therefore have equal heat inputs.

a. Earth Emitted Heat Inputs.

Figure 15 shows the Earth emitted heat flux to SOEP 1 and 2.

b. Direct Solar Heat Inputs.

The direct solar input to SOEP 1 and 2 is constant (137.4 milliwatts/cm²) since it is controlled to point toward the Sun. Figure 16 shows that the satellite did not go into an eclipse during this particular time period, since the curve is continuous.

c. Reflected Solar Heat Inputs.

Figure 17 presents a comparison between the exact and approximate values of the reflected solar heat inputs to SOEP 1 and 2. Figure 17 shows that the largest difference between the exact and approximate values is 1.22 milliwatts/cm².

3. The Orbit Plane Experiment Packages.

The orbit plane experiment packages (OPEP 1 and OPEP 2) are controlled so that their normals lie in the orbit plane and such that the angle between their normals and the vehicle velocity vector is less than 90° (or $\bar{n} \cdot \dot{\bar{r}}_{VE} > 0$).

a. Earth Emitted Heat Inputs

Figure 18 presents the Earth emitted heat inputs to OPEP 1 and 2. The values are equal since both OPEP normals point in the same direction.

b. Direct Solar Heat Inputs

Figure 19 presents the direct solar heat inputs to OPEP 1 and OPEP 2. The two experiments have the same inputs except for shadowing of the OPEPs by the main box. This figure shows that OPEP 2 has no solar heat input from 0. to 32.5 hours from perigee. It also indicates that OPEP 2 is shadowed from the Sun by the main box. OPEP 1 becomes shadowed by the main box at 42.5 hours.

c. Reflected Solar Heat Inputs

Figure 20 presents a comparison between the exact and approximate values of the reflected solar heat inputs to OPEP 1 and 2. OPEP 1 and 2 have equal inputs since they have equal normals. The largest difference between the exact and approximate values is 0.73 milliwatts/cm².

VII REFERENCES

1. Shaffer, F., Squires, R. K., Wolf, H., Interplanetary Trajectory Encke Method (ITEM), NASA Report X640-63-71, Goddard Space Flight Center, Greenbelt, Maryland.
2. Hemenover, A. D., Nominal Trajectory and Impact Data of EOGO, Lockheed Missiles and Space Company, Report No. A-306775/91-21, dated November 9, 1962, Sunnyvale, California.
3. Space Technology Laboratories, Inc. letter number 8100.2-541, dated 21 August 1962, letter from John W. Linden to W. E. Scull.
4. STL Drawing, Number 100005, General Arrangement of OGO, Shakespear, W., October 12, 1961, Space Technology Laboratories, Inc., Redondo Beach, California.
5. Montgomery, H. E., Paddack, S. J., S-49, EGO Launch Window and Orbit, NASA Report X640-63-119, Goddard Space Flight Center, Greenbelt, Maryland.
6. Otten, D. D., OGO Attitude Control Subsystem Description, Logic and Specifications, Report Number 2313-0004-RV-000, 4 December, 1961, Space Technology Laboratories, Inc. Redondo Beach, California.

7. Allen, C. W., Astrophysical Quantities, University of London, The Athlone Press, 1955, Published in U.S.A. by Essential Books, Fairlawn, New Jersey.
8. Montgomery, H. E., and Paddack, S. J., EGO Orbital Parameters and Heat Inputs, NASA Report Number X-643-63-61, Goddard Space Flight Center, Greenbelt, Maryland.

APPENDIX A

The Equation of a Plane

Equations (1) and (2) in Section IV-B show a fourth order determinant and the analytical expression of a plane surface. The determinant and its relation to the analytical expression are shown here.

Let $\bar{r}_l, \bar{r}_m, \bar{r}_n$ be vectors in an orthogonal coordinate system which are directed to any three vertices of a plane surface.

If $\bar{i}, \bar{j}, \bar{k}$ are unit vectors along the x, y, z axes respectively $\bar{r}_l, \bar{r}_m, \bar{r}_n$ can be expressed as:

$$\begin{aligned}\bar{r}_l &= \bar{i}x_l + \bar{j}y_l + \bar{k}z_l \\ \bar{r}_m &= \bar{i}x_m + \bar{j}y_m + \bar{k}z_m \\ \bar{r}_n &= \bar{i}x_n + \bar{j}y_n + \bar{k}z_n \\ \bar{r} &= \bar{i}x + \bar{j}y + \bar{k}z\end{aligned}\tag{A-1}$$

Where \bar{r} is any vector from the origin to the plane surface. Vector subtraction forms the vectors $\bar{u}, \bar{v}, \bar{w}$ in the plane:

$$\begin{aligned}\bar{u} &= \bar{r} - \bar{r}_l = (x - x_l)\bar{i} + (y - y_l)\bar{j} + (z - z_l)\bar{k} \\ \bar{v} &= \bar{r} - \bar{r}_m = (x - x_m)\bar{i} + (y - y_m)\bar{j} + (z - z_m)\bar{k} \\ \bar{w} &= \bar{r} - \bar{r}_n = (x - x_n)\bar{i} + (y - y_n)\bar{j} + (z - z_n)\bar{k}\end{aligned}\tag{A-2}$$

Since \bar{u} , \bar{v} , \bar{w} are coplanar their triple scalar product is equal to zero.

$$(\bar{u} \times \bar{v}) \cdot \bar{w} = \begin{vmatrix} u_x & u_y & u_z \\ v_x & v_y & v_z \\ w_x & w_y & w_z \end{vmatrix} = 0 \quad (\text{A-3})$$

Where the elements of the determinant are the coefficients of \bar{i} , \bar{j} , \bar{k} in equation (A-2). Hence

$$\begin{vmatrix} (x - x_l) & (y - y_l) & (z - z_l) \\ (x - x_m) & (y - y_m) & (z - z_m) \\ (x - x_n) & (y - y_n) & (z - z_n) \end{vmatrix} = 0 \quad (\text{A-4})$$

The above determinant may be expanded to:

$$\begin{vmatrix} x & y & z \\ -x_m & -y_m & -z_m \\ -x_n & -y_n & -z_n \end{vmatrix} + \begin{vmatrix} -x_l & -y_l & -z_l \\ x & y & z \\ -x_n & -y_n & -z_n \end{vmatrix} + \begin{vmatrix} -x_l & -y_l & -z_l \\ -x_m & -y_m & -z_m \\ x & y & z \end{vmatrix} + \begin{vmatrix} -x_l & -y_l & -z_l \\ -x_m & -y_m & -z_m \\ -x_n & -y_n & -z_n \end{vmatrix} = 0 \quad (\text{A-5})$$

Factoring out -1 from the l, m, n rows of each of the above determinants and interchanging the rows for symmetry yields:

$$\begin{vmatrix} x & y & z \\ x_m & y_m & z_m \\ x_n & y_n & z_n \end{vmatrix} - \begin{vmatrix} x & y & z \\ x_l & y_l & z_l \\ x_n & y_n & z_n \end{vmatrix} + \begin{vmatrix} x & y & z \\ x_l & y_l & z_l \\ x_m & y_m & z_m \end{vmatrix} - \begin{vmatrix} x_l & y_l & z_l \\ x_m & y_m & z_m \\ x_n & y_n & z_n \end{vmatrix} = 0 \quad (\text{A-6})$$

The determinants of equation (A-6) can be considered the minors of an expanded fourth order determinant which has been expanded for a column whose elements are unity.

$$\begin{vmatrix} x & y & z & 1 \\ x_l & y_l & z_l & 1 \\ x_m & y_m & z_m & 1 \\ x_n & y_n & z_n & 1 \end{vmatrix} = 0 \quad (\text{A-7})$$

Hence, the expression of a plane is described as a fourth order determinant.

Expanding equation (A-7) for the elements of the first row produces:

$$\begin{aligned}
 & x \begin{vmatrix} y_l & z_l & 1 \\ y_m & z_m & 1 \\ y_n & z_n & 1 \end{vmatrix} - y \begin{vmatrix} x_l & z_l & 1 \\ x_m & z_m & 1 \\ x_n & z_n & 1 \end{vmatrix} + \\
 & z \begin{vmatrix} x_l & y_l & 1 \\ x_m & y_m & 1 \\ x_n & y_n & 1 \end{vmatrix} - 1 \begin{vmatrix} x_l & y_l & z_l \\ x_m & y_m & z_m \\ x_n & y_n & z_n \end{vmatrix} = 0 \quad (A-8)
 \end{aligned}$$

Letting the minors of x, y, z, 1 equal A, B, C, D respectively the analytical expression of a plane surface can be written.

$$Ax + By + Cz + D = 0$$

Accordingly, any plane surface can be described by the proper choice of A, B, C, D. For instance the i^{th} surface is:

$$A_i x + B_i y + C_i z + D_i = 0 \quad (A-9)$$

or in other words the four vector, (A_i, B_i, C_i, D_i) describes the i^{th} surface. Since a triple scalar product can be written as a third order determinant, the coefficients of the analytical expression for a plane

surface can be written as:

$$\begin{aligned}
 A_i &= \begin{vmatrix} y_l & z_l & 1 \\ y_m & z_m & 1 \\ y_n & z_n & 1 \end{vmatrix} = \bar{U} \cdot (\bar{Y}_{lmn} \times \bar{Z}_{lmn}) \\
 B_i &= - \begin{vmatrix} x_l & z_l & 1 \\ x_m & z_m & 1 \\ x_n & z_n & 1 \end{vmatrix} = \bar{U} \cdot (\bar{Z}_{lmn} \times \bar{X}_{lmn}) \\
 C_i &= \begin{vmatrix} x_l & y_l & 1 \\ x_m & y_m & 1 \\ x_n & y_n & 1 \end{vmatrix} = \bar{U} \cdot (\bar{X}_{lmn} \times \bar{Y}_{lmn}) \\
 D_i &= - \begin{vmatrix} x_l & y_l & z_l \\ x_m & y_m & z_m \\ x_n & y_n & z_n \end{vmatrix} = -\bar{X}_{lmn} (\bar{Y}_{lmn} \times \bar{Z}_{lmn})
 \end{aligned} \tag{A-10}$$

where

$$\begin{aligned}
 \bar{X}_{lmn} &\equiv (x_l, x_m, x_n) \\
 \bar{Y}_{lmn} &\equiv (y_l, y_m, y_n) \\
 \bar{Z}_{lmn} &\equiv (z_l, z_m, z_n) \\
 \bar{U} &\equiv (1, 1, 1)
 \end{aligned} \tag{A-11}$$

The right hand sides of these definitions are three-vectors.

APPENDIX B

The sign of a mathematical expression may be used to determine whether any two points are on the same or opposite sides of a plane surface.

$$(\bar{S}_i \cdot \bar{R}_j)(\bar{S}_i \cdot \bar{R}_k) = s \quad \text{Equation (10), Section IV}$$

where

$\bar{S}_i \equiv (A_i, B_i, C_i, D_i)$ is a four-vector denoting the analytic representation of a plane containing the i^{th} face. (See Appendix A).

$\bar{R}_j \equiv (x_j, y_j, z_j, 1)$ is a four-vector denoting the position of the Sun.

$\bar{R}_k \equiv (x_k, y_k, z_k, 1)$ is a four-vector denoting the position of an experiment package.

if

$s > 0$ then \bar{R}_j and \bar{R}_k are on the same side of \bar{S}_i .

$s < 0$ then \bar{R}_j and \bar{R}_k are on opposite sides of \bar{S}_i .

$s = 0$ then either \bar{R}_j or \bar{R}_k , or both are in the plane of \bar{S}_i .

In general, to determine the relative positions of two points in space with respect to a surface it is sufficient to establish the angles

between a normal vector to the surface and the position vectors measured from the surface to the points.

Graphically this may be represented (See Figure B-1), where

\bar{n} = normal vector

\bar{q}_j = vector from the surface to \bar{r}_j

\bar{q}_k = vector from the surface to \bar{r}_k

\bar{r}_j = position vector of the Sun

$$= x_j \bar{i} + y_j \bar{j} + z_j \bar{k}$$

\bar{r}_k = position vector of an experiment package

$$= x_k \bar{i} + y_k \bar{j} + z_k \bar{k}$$

\bar{r} = vector to origin of \bar{n}

$$= x \bar{i} + y \bar{j} + z \bar{k}$$

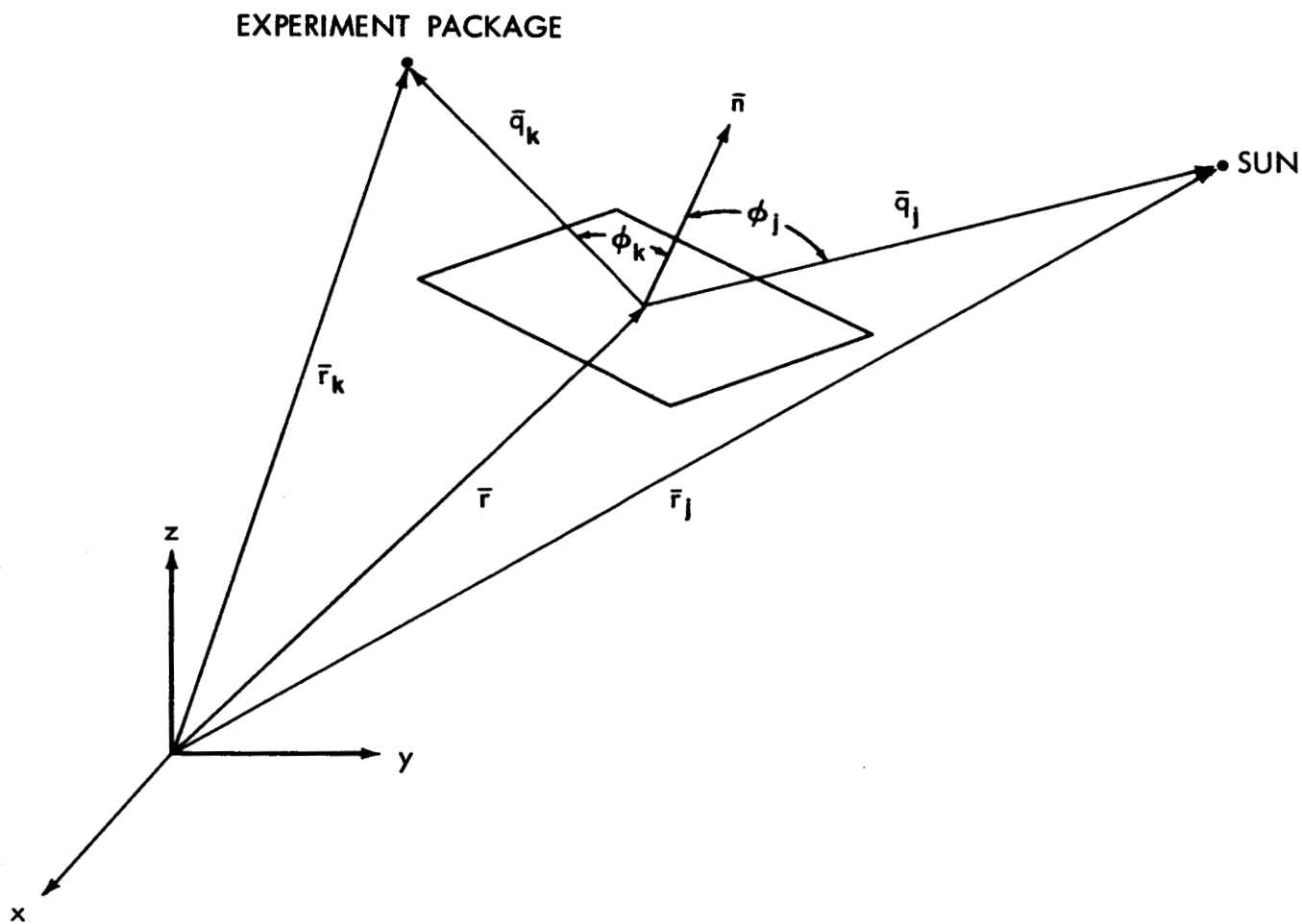
ϕ_j = angle between \bar{n} and \bar{q}_j

ϕ_k = angle between \bar{n} and \bar{q}_k

Note that \bar{n} , \bar{q}_j , \bar{q}_k , \bar{r}_j , \bar{r}_k and \bar{r} are all three-vectors (i. e. defined in 3-dimensional orthogonal space), and that

$$\bar{r}_j \neq \bar{R}_j$$

$$\bar{r}_k \neq \bar{R}_k$$



Based on these definitions the following relationships are made:

CASE	ϕ_j	ϕ_k	SIGN OF $\bar{n} \cdot \bar{q}_j$	SIGN OF $\bar{n} \cdot \bar{q}_k$	SIGN OF $\left(\bar{n} \cdot \bar{q}_j\right) \times$ $\left(\bar{n} \cdot \bar{q}_k\right)$	RELATION OF \bar{q}_j and \bar{q}_k
1	$\phi_j < \pi/2$	$\phi_k < \pi/2$	+	+	+	same side
2	$\phi_j > \pi/2$	$\phi_k < \pi/2$	-	+	-	opposite sides
3	$\phi_j < \pi/2$	$\phi_k > \pi/2$	+	-	-	opposite sides
4	$\phi_j > \pi/2$	$\phi_k > \pi/2$	-	-	+	same side

This table may be summarized in one mathematical expression,

$$\left(\bar{n} \cdot \bar{q}_j\right) \left(\bar{n} \cdot \bar{q}_k\right) = s \quad (B-1)$$

When $s > 0$, \bar{q}_j and \bar{q}_k are on the same side of the surface.

When $s < 0$, \bar{q}_j and \bar{q}_k are on opposite sides of the surface.

In order to prove that the sign of $\left(\bar{S}_i \cdot \bar{R}_j\right) \left(\bar{S}_i \cdot \bar{R}_k\right)$ yields the same information as $\left(\bar{n} \cdot \bar{q}_j\right) \left(\bar{n} \cdot \bar{q}_k\right)$ it is necessary to show the relationship between the two expressions.

$$A_i x + B_i y + C_i z + D_i = 0 \text{ (equation of plane surface)}$$

$$\nabla(A_i x + B_i y + C_i z + D_i) = \text{normal to plane surface} \quad (B-2)$$

$$\nabla(A_i x + B_i y + C_i z + D_i) = A_i \bar{i} + B_i \bar{j} + C_i \bar{k}$$

Hence,

$$\bar{n} \equiv A_i \bar{i} + B_i \bar{j} + C_i \bar{k}$$

From the figure above it can be seen that

$$\bar{q}_j = \bar{r}_j - \bar{r}$$

$$\bar{q}_k = \bar{r}_k - \bar{r}$$

These substituted into equation (B-1) yield:

$$[\bar{n} \cdot (\bar{r}_j - \bar{r})][\bar{n} \cdot (\bar{r}_k - \bar{r})] = s$$

$$[(\bar{n} \cdot \bar{r}_j) - (\bar{n} \cdot \bar{r})][(\bar{n} \cdot \bar{r}_k) - (\bar{n} \cdot \bar{r})] = s$$

$$\left[(A_i x_j + B_i y_j + C_i z_j) - (A_i x + B_i y + C_i z) \right] x$$

$$\left[(A_i x_k + B_i y_k + C_i z_k) - (A_i x + B_i y + C_i z) \right] = s$$

Since

$$-D_i = A_i x + B_i y + C_i z$$

Hence

$$(A_i x_j + B_i y_j + C_i z_j + D_i)(A_i x_k + B_i y_k + C_i z_k + D_i) = s \quad (B-3)$$

Defining

$$\bar{R}_j \equiv (x_j, y_j, z_j, 1)$$

$$\bar{R}_k \equiv (x_k, y_k, z_k, 1)$$

and noting that

$$\bar{S}_i \equiv (A_i, B_i, C_i, D_i)$$

Equation (B-3) can be written as

$$(\bar{S}_i \cdot \bar{R}_j)(\bar{S}_i \cdot \bar{R}_k) = s$$

Hence, it is shown that the sign of this expression (which is identical to equation (10), Section IV) is a valid means of determining whether any two points are on the same or opposite sides of a plane surface.

APPENDIX C

The Equation of a Straight Line

The projections of the vertices of a polygonal face onto the test plane (See Figure C-1) are given by:

$$\bar{p}_j'' = x_j'' \bar{i}'' + y_j'' \bar{j}'' \quad (C-1)$$

The line connecting two successive vertices, \bar{p}_j'' and \bar{p}_{j+1}'' can be represented by the vector difference of these two vertices.

$$\bar{l}_{j,j+1} = \bar{p}_j'' - \bar{p}_{j+1}'' \quad (C-2)$$

$$\bar{l}_{j,j+1} = (x_j'' - x_{j+1}'') \bar{i}'' + (y_j'' - y_{j+1}'') \bar{j}'' \quad (C-3)$$

Since the above expression is the equation of a straight line of the form

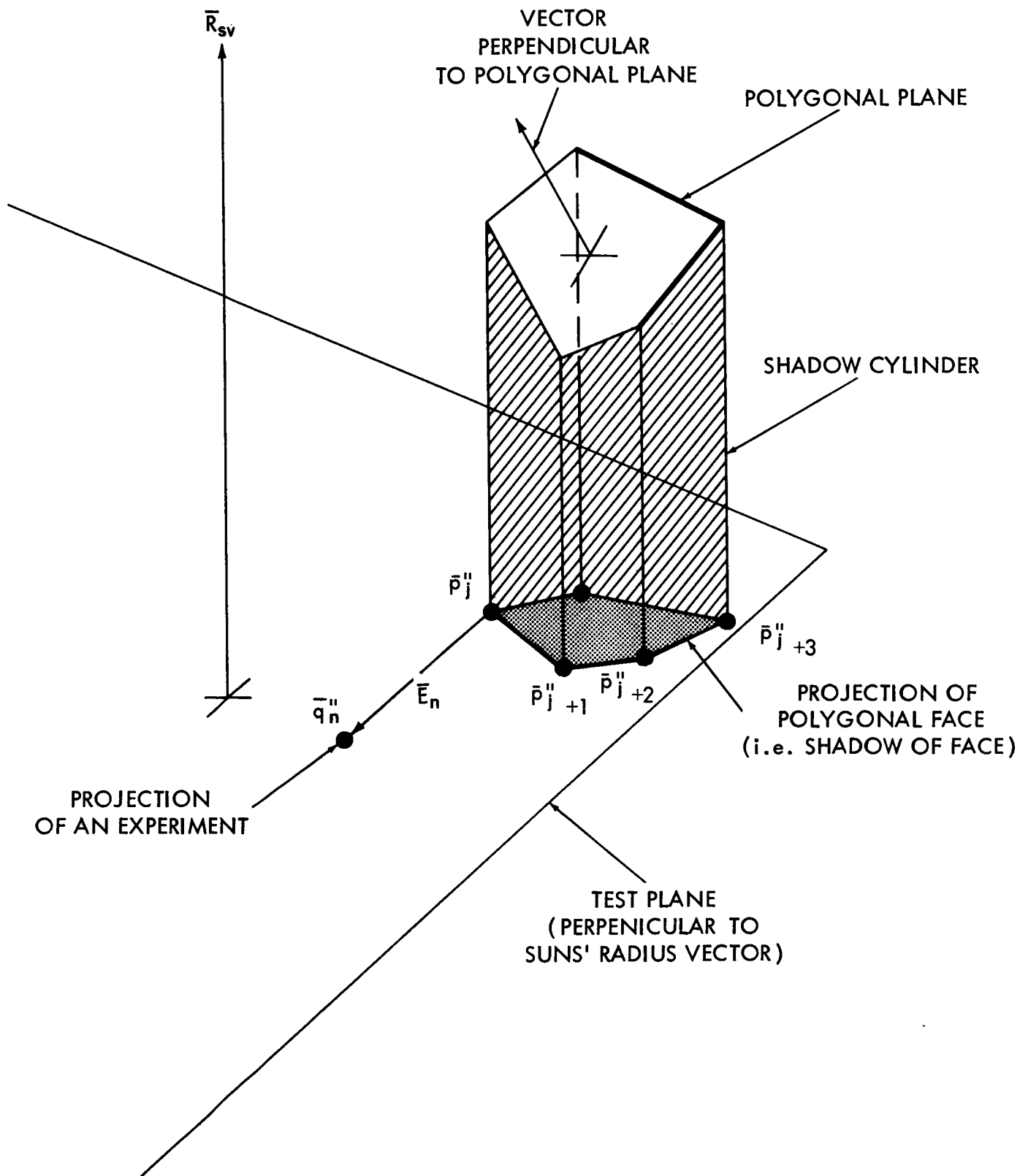
$$ax'' + by'' + c = 0$$

where $-a/b$ is the slope of the line. Hence, the slope of $\bar{l}_{j,j+1}$ is:

$$\text{Slope} = \frac{(y_j'' - y_{j+1}'')}{(x_j'' - x_{j+1}'')} \quad (C-4)$$

The slope of any straight line is the same anywhere along the line, consequently:

$$\frac{y_j'' - y_{j+1}''}{x_j'' - x_{j+1}''} = \frac{y'' - y_j''}{x'' - x_j''} \quad (C-5)$$



Expanding yields:

$$-(x_j'' - x_{j+1}'')(y_j'' - y_{j+1}'') + (x'' - x_j'')(y_j'' - y_{j+1}'') = 0$$

$$-x_j'' y'' + x_j'' y_j'' + x_{j+1}'' y'' - x_{j+1}'' y_j'' + x'' y_j'' - x'' y_{j+1}'' - x_j'' y_j'' + x_j'' y_{j+1}'' = 0$$

The above equation can be written in terms of determinants:

$$\begin{vmatrix} x_j'' & y_j'' \\ x_{j+1}'' & y_{j+1}'' \end{vmatrix} - \begin{vmatrix} x'' & y'' \\ x_{j+1}'' & y_{j+1}'' \end{vmatrix} + \begin{vmatrix} x'' & y'' \\ x_j'' & y_j'' \end{vmatrix} = 0 \quad (C-6)$$

The determinants of equation C-6 can be considered the minors of an expanded third order determinant which has been expanded for a column whose elements are unity.

$$\begin{vmatrix} x'' & y'' & 1 \\ x_j'' & y_j'' & 1 \\ x_{j+1}'' & y_{j+1}'' & 1 \end{vmatrix} = 0 \quad (C-7)$$

Expanding equation C-7 for the elements of the first row produces:

$$x''(y_j'' - y_{j+1}'') - y''(x_j'' - x_{j+1}'') + (x_j'' y_{j+1}'' - x_{j+1}'' y_j'') = 0 \quad (C-8)$$

Letting

$$a_j = y_j'' - y_{j+1}''$$

$$b_j = -x_j'' + x_{j+1}''$$

$$c_j = x_j'' y_{j+1}'' - x_{j+1}'' y_j''$$

Hence, the familiar straight line formula:

$$a_j x'' + b_j y'' + c_j = 0 \quad (C-9)$$

This equation can be considered the result of a dot product of two three-vectors:

$$\bar{L}_{j,j+1} \equiv (a_j, b_j, c_j) \quad (C-10)$$

$$\bar{P} = (x'', y'', 1) \quad (C-11)$$

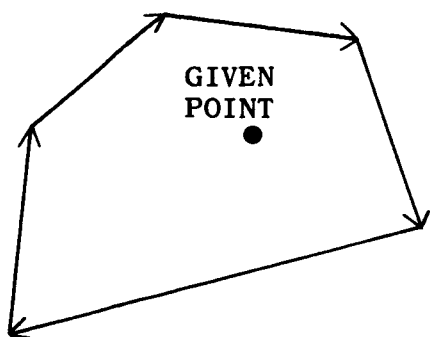
$$\bar{L}_{j,j+1} \cdot \bar{P} = a_j x'' + b_j y'' + c_j = 0 \quad (C-12)$$

APPENDIX D

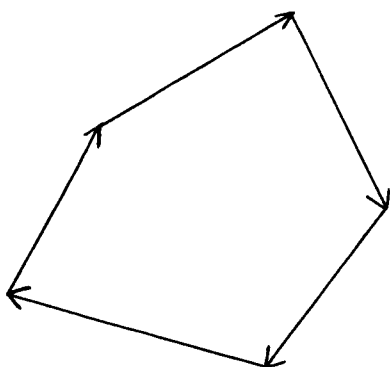
The Shadow Test

In order to test whether or not an experiment is in the shadow of the satellite the experiment is investigated with respect to each surface of the satellite and to the cylindrical projected shadows from each of these surfaces. The polygonal surface and the experiments are projected onto a test plane which is perpendicular to the Sun's light rays. (See Figure C-1, p. C-2.) If a given point on the test plane (i. e. the projection of an experiment onto the test plane lies within the boundaries of the polygonal shadow on that plane the experiment will necessarily have to be in the cylindrical shadow since the Sun and experiment are on opposite sides of the satellite surface. If the boundary of the polygonal shadow is described by a series of vectors $\vec{l}_{j,j+1}$ where $j = 0, 1, 2, \dots, M - 1$ for an M sided polygon connected tip to tail in clockwise fashion and if the given point lies on the right hand side of each of these boundary-describing vectors the given point must lie within the boundary. If the point lies to the left of any side of the polygon the point cannot be within the boundary and hence is not in the shadow of that surface of the satellite.

Graphically this may be represented as:



In this case the given point lies to the right of each vector and the experiment is in the shadow.



● Given Point

In this case the given point lies to the right of some but not all of the boundary describing vectors and hence the experiment is not in the shadow of the surface causing this polygonal shadow. It may be in the shadow of another surface.

The sides of the polygon are represented by:

$$\vec{l}_{j,j+1} = \vec{p}_{j+1}'' - \vec{p}_j'' \quad (\text{See Appendix C})$$

where

$$j = 0, 1, 2, \dots, M-1$$

M = number of sides on polygon

and

$$\vec{p}_0'' = (0, 0, 0,)$$

The vector \bar{q}_n'' is the projection of an experiment package on the test plane in the \bar{p}_j'' system.

Let

$$\bar{E}_n = \bar{q}_n'' - \bar{p}_j'' \text{ (See Figure C-1 page C-2)}$$

and also let

$$\bar{\xi} = (\bar{p}_{j+2}'' - \bar{p}_j'') \times \bar{l}_{j,j+1}$$

$$\bar{M} = \bar{l}_{j,j+1} \times \bar{\xi}$$

\bar{M} lies in the plane of the polygon and is perpendicular to $\bar{l}_{j,j+1}$. If $\bar{M} \cdot \bar{E}_n > 0$ for all j from 0 to $M-1$ the experiment projection will lie to the right hand side of each $\bar{l}_{j,j+1}$ and consequently in the polygonal shadow. If for any j , $\bar{M} \cdot \bar{E}_n \leq 0$ the experiment projection cannot lie within the polygonal shadow and consequently the experiment package cannot be in the cylindrical shadow projected from the polygon in space. It is shown here that

$$\bar{M} \cdot \bar{E}_n = (\bar{Q}_n \cdot \bar{l}_{j,j+1}) (\bar{P}_{j+2} \cdot \bar{l}_{j,j+1})$$

Where

$$\bar{Q}_n, \bar{l}_{j,j+1} \text{ and } \bar{P}_{j+2}$$

are three-vectors defined on page D-6.

$$\bar{l}_{j,j+1} = \bar{p}_{j+1}'' - \bar{p}_j'' = (x_{j+1}'' - x_j'') \bar{i}'' + (y_{j+1}'' - y_j'') \bar{j}'' \quad (D-1)$$

$$(\bar{r}_{j+2}'' - \bar{r}_j'') = (x_{j+2}'' - x_j'') \bar{i}'' + (y_{j+2}'' - y_j'') \bar{j}'' \quad (D-2)$$

$$\bar{E}_n = \bar{q}_n'' - \bar{p}_j'' = (x_n'' - x_j'') \bar{i}'' + (y_n'' - y_j'') \bar{j}'' \quad (D-3)$$

$$(\bar{r}_{j+2}'' - \bar{r}_j'') \times \bar{l}_{j,j+1} = \begin{vmatrix} \bar{i}'' & \bar{j}'' & \bar{k}'' \\ (x_{j+2}'' - x_j'') & (y_{j+2}'' - y_j'') & 0 \\ (x_{j+1}'' - x_j'') & (y_{j+1}'' - y_j'') & 0 \end{vmatrix} = |\bar{\xi}| \quad (D-4)$$

$$\bar{\xi} = \left\{ (x_{j+2}'' - x_j'') (y_{j+1}'' - y_j'') - (x_{j+1}'' - x_j'') (y_{j+2}'' - y_j'') \right\} \bar{k}'' = |\bar{\xi}| \bar{k}'' \quad (D-5)$$

$$\bar{l}_{j,j+1} \times \bar{\xi} = \begin{vmatrix} \bar{i}'' & \bar{j}'' & \bar{k}'' \\ (x_{j+1}'' - x_j'') & (y_{j+1}'' - y_j'') & 0 \\ 0 & 0 & |\bar{\xi}| \end{vmatrix} = \bar{M} \quad (D-6)$$

$$\bar{M} = (y_{j+1}'' - y_j'') |\bar{\xi}| \bar{i}'' - (x_{j+1}'' - x_j'') |\bar{\xi}| \bar{j}'' \quad (D-7)$$

$$\bar{M} \cdot \bar{E}_n = (x_n'' - x_j'') (y_{j+1}'' - y_j'') |\bar{\xi}| - (y_n'' - y_j'') (x_{j+1}'' - x_j'') |\bar{\xi}| \quad (D-8)$$

$$= |\bar{\xi}| \left\{ (x_n'' - x_j'') (y_{j+1}'' - y_j'') - (y_n'' - y_j'') (x_{j+1}'' - x_j'') \right\} \quad (D-9)$$

But

$$a_j = y_j'' - y_{j+1}''$$

$$b_j = -x_j'' + x_{j+1}''$$

(See Appendix C)

Hence:

$$\begin{aligned}
\bar{\mathbf{M}} \cdot \bar{\mathbf{E}}_n &= \left\{ (x_{j+2}'' - x_j'') a_j + (y_{j+2}'' - y_j'') b_j \right\} \\
&\quad \left\{ (x_n'' - x_j'') a_j + (y_n'' - y_j'') b_j \right\} \\
&= \left\{ a_j x_{j+2}'' - a_j x_j'' + b_j y_{j+2}'' - b_j y_j'' \right\} \\
&\quad \left\{ a_j x_n'' - a_j x_j'' + b_j y_n'' - b_j y_j'' \right\} \tag{D-10} \\
&= \left\{ a_j x_{j+2}'' + b_j y_{j+2}'' - x_j'' y_{j+1}'' + x_{j+1}'' y_j'' \right\} \\
&\quad \left\{ a_j x_n'' + b_j y_n'' - x_j'' y_{j+1}'' + x_{j+1}'' y_j'' \right\}
\end{aligned}$$

Since

$$c_j = x_j'' y_{j+1}'' - x_{j+1}'' y_j'' \quad (\text{See Appendix C})$$

$$\bar{\mathbf{M}} \cdot \bar{\mathbf{E}}_n = (a_j x_{j+2}'' + b_j y_{j+2}'' + c_j) (a_j x_n'' + b_j y_n'' + c_j) \tag{D-11}$$

The above expression can be thought of as the product of two dot products:

$$\bar{\mathbf{M}} \cdot \bar{\mathbf{E}}_n = \left[(a_j, b_j, c_j) \cdot (x_{j+2}'', y_{j+2}'', 1) \right] \left[(a_j, b_j, c_j) \cdot (x_n'', y_n'', 1) \right] \tag{D-12}$$

This can be written as:

$$\bar{\mathbf{M}} \cdot \bar{\mathbf{E}}_n = (\bar{\mathbf{L}}_{j, j+1} \cdot \bar{\mathbf{P}}_{j+2}) (\bar{\mathbf{L}}_{j, j+1} \cdot \bar{\mathbf{Q}}_n) \tag{D-13}$$

Where

$\bar{L}_{j,j+1} \equiv (a_j, b_j, c_j)$ is a three-vector denoting the analytical expression of a line which is a boundary of the polygonal shadow of a surface of the satellite.

$\bar{P}_{j+2} \equiv (x_{j+2}'', y_{j+2}'', 1)$ is a three-vector denoting the position of the \bar{p}_{j+2}'' vertex.

$\bar{Q}_n \equiv (x_n'', y_n'', 1)$ is a three-vector denoting the position of the projection of the n th experiment on the test plane.

Hence the test can be written as:

$$(\bar{Q}_n \cdot \bar{L}_{j,j+1})(\bar{P}_{j+2} \cdot \bar{L}_{j,j+1}) > 0 \quad (D-14)$$

for all $j = 0, 1, 2 \dots M-1$. This is identically equal to equation (22) in Section IV B. The derivation shown in this appendix proves that equation (22) is a valid means of determining whether or not an experiment is in the shadow of a plane surface in space (i. e. a component part of a satellite) providing that the Sun and experiment are on opposite sides of the plane surface in space.

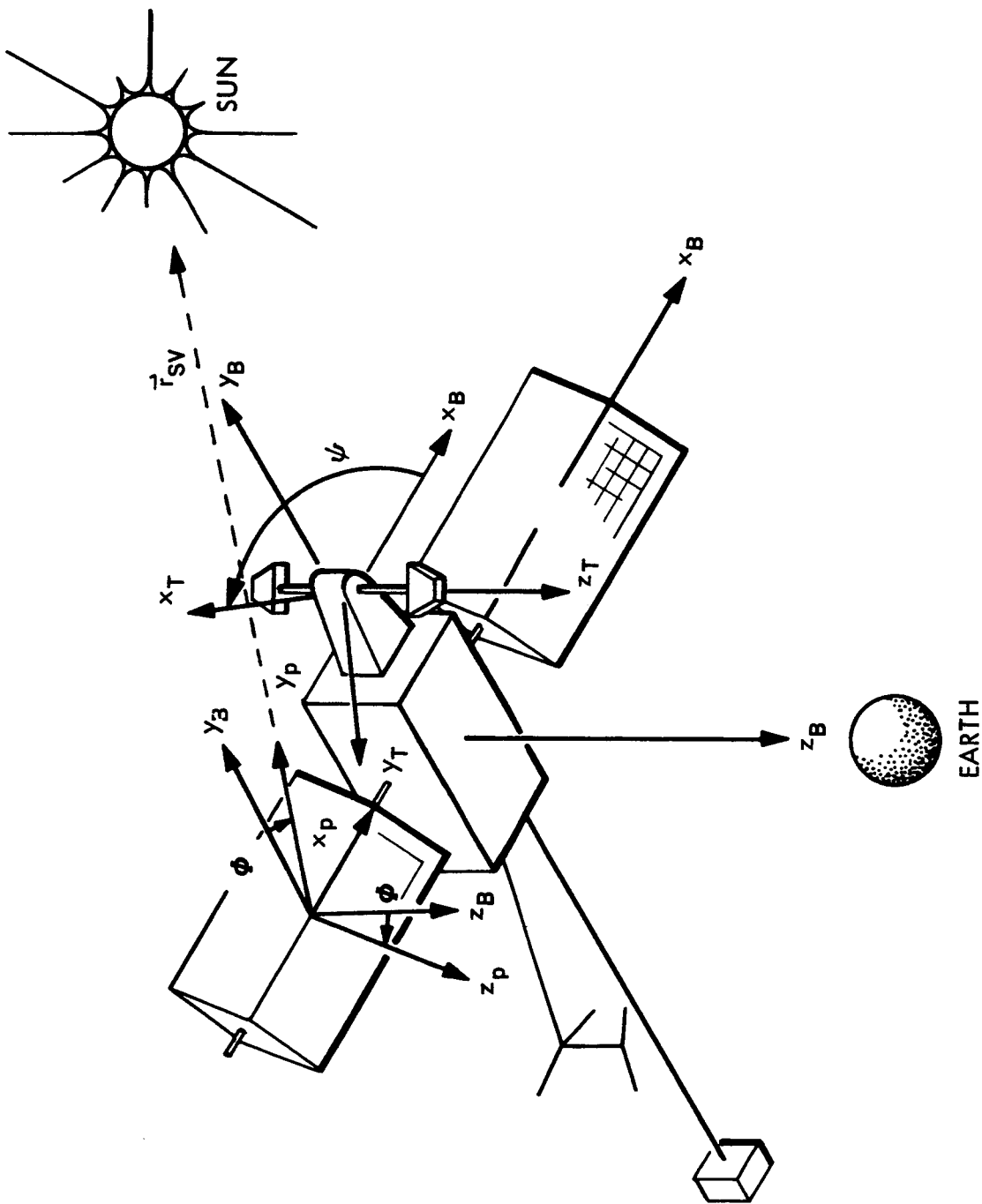


Figure 1—Body Coordinate System.

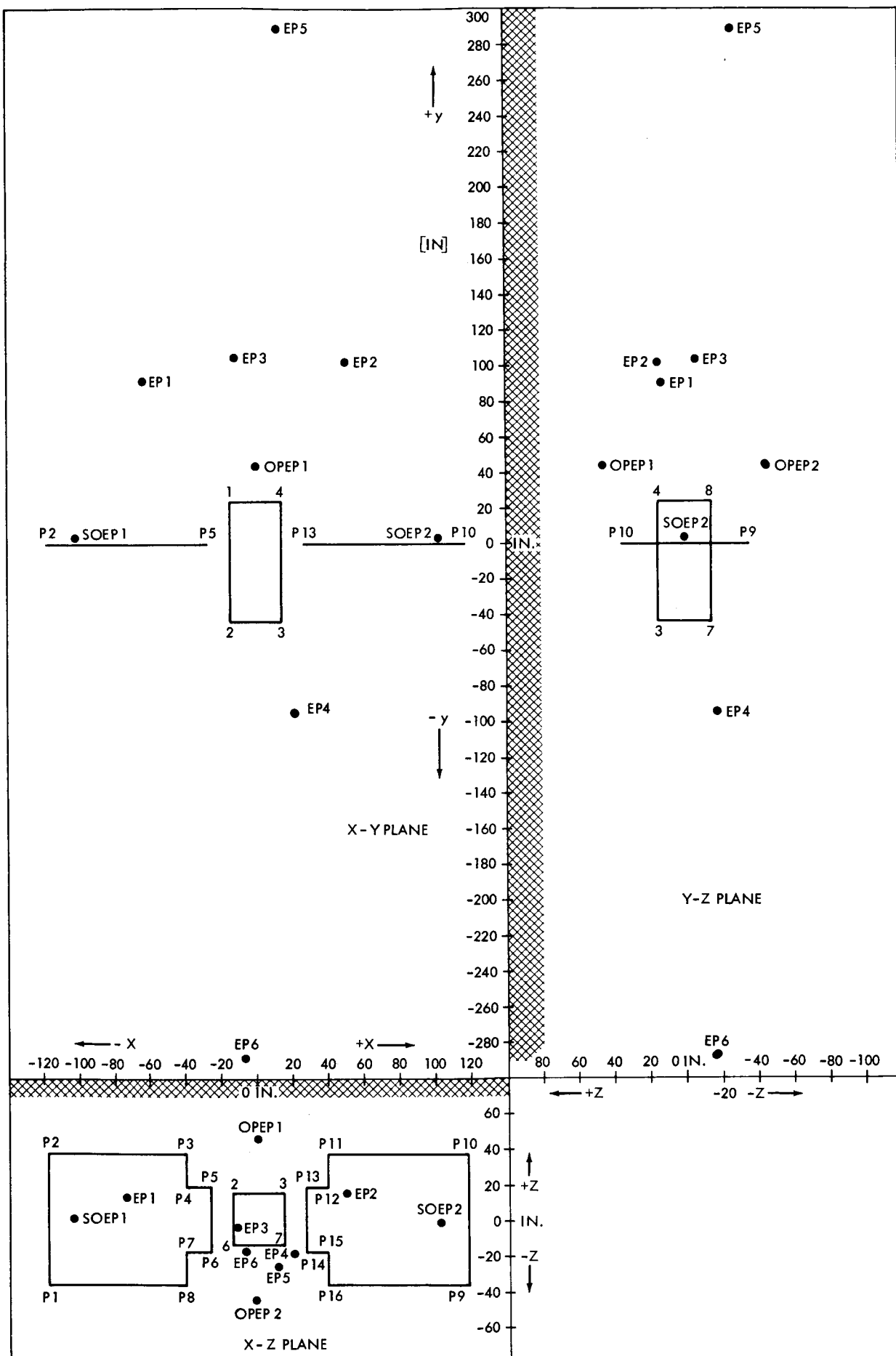


FIG. 2 S-49 EGO SATELLITE GEOMETRY

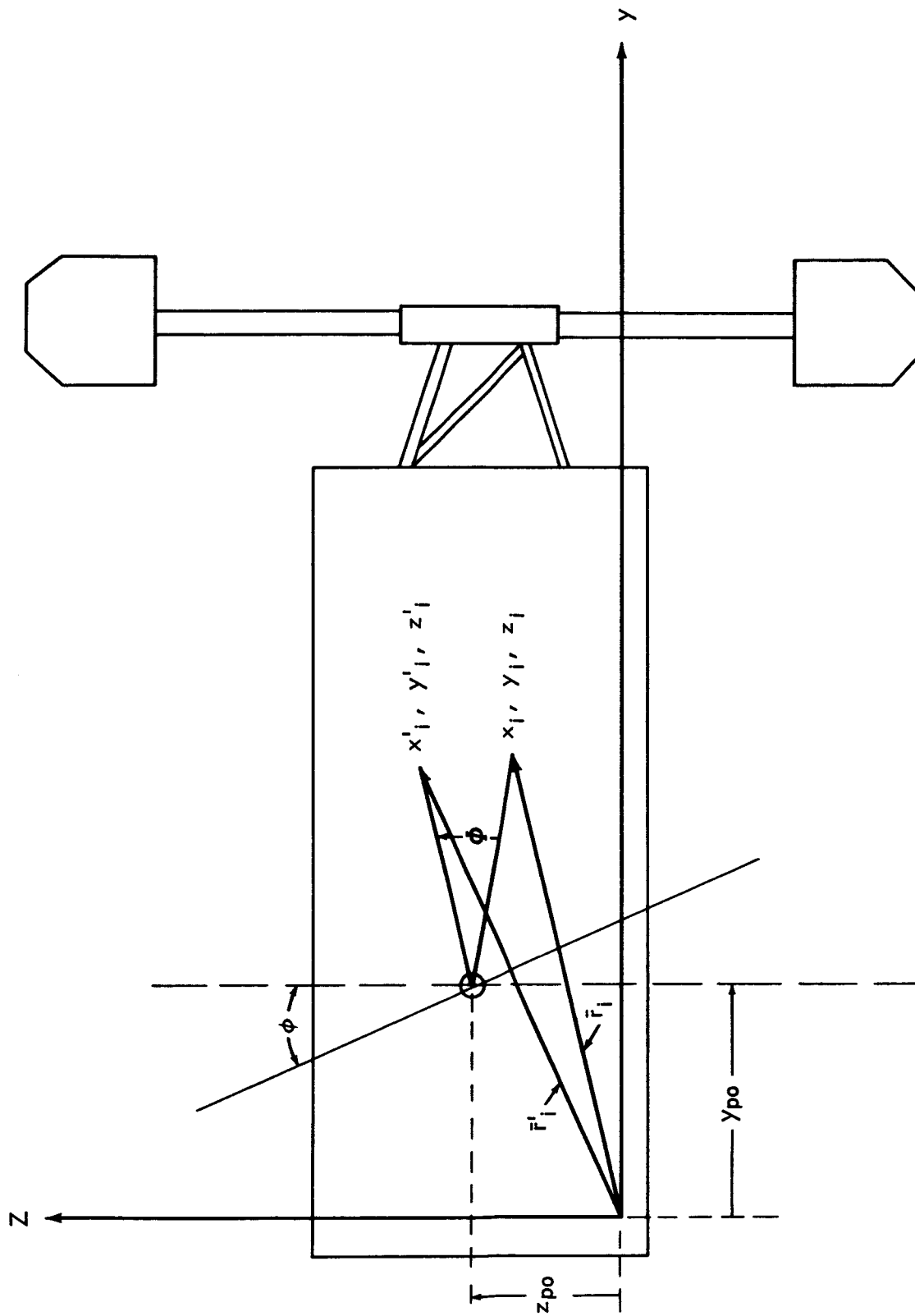


Figure 3--Coordinate System for Solar Array.

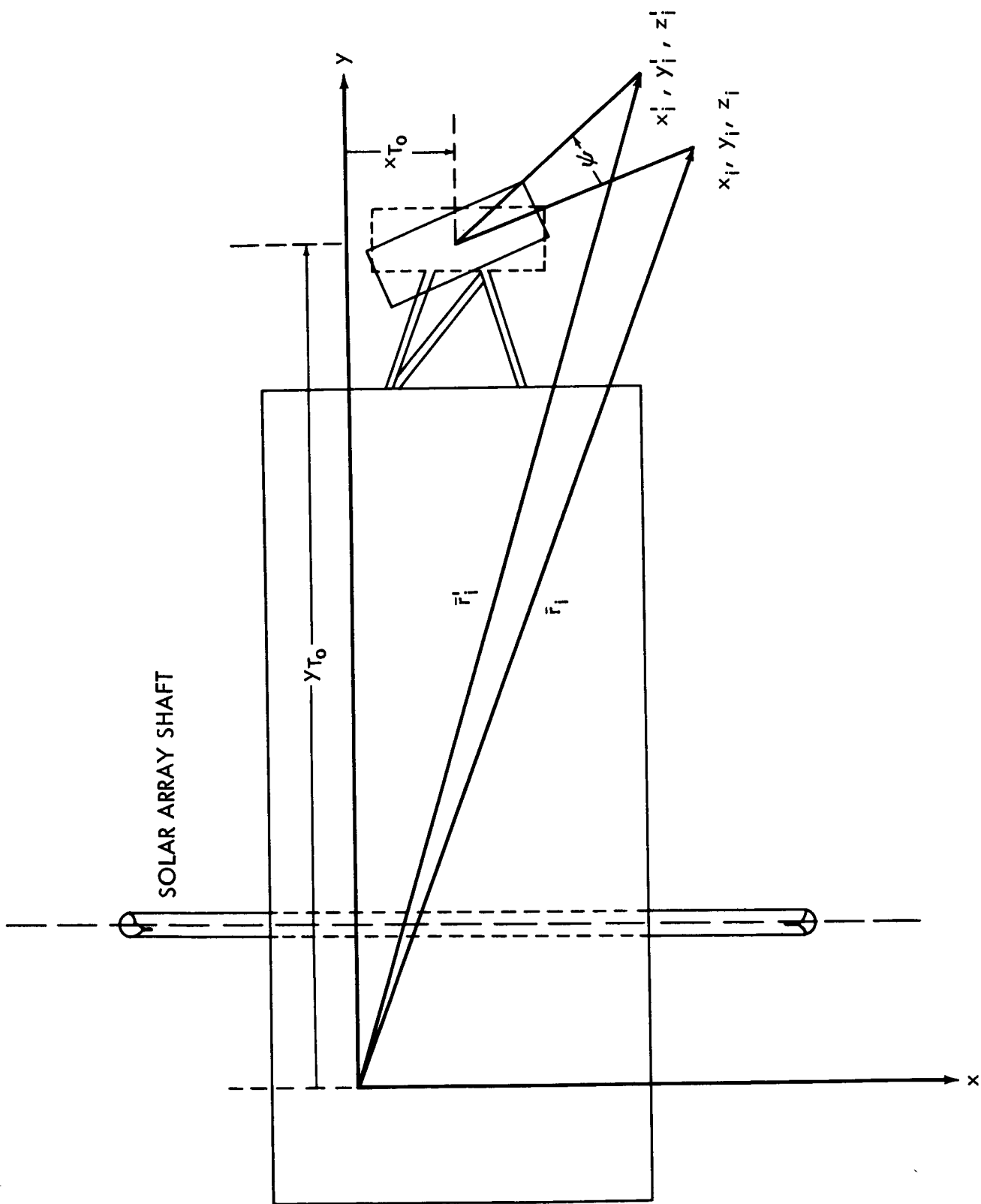


Figure 4--Coordinate System for OPEP.

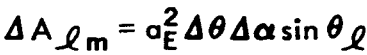


Figure 5—Geometry for Heat Inputs.

MAIN BOX SHADOW HISTORY

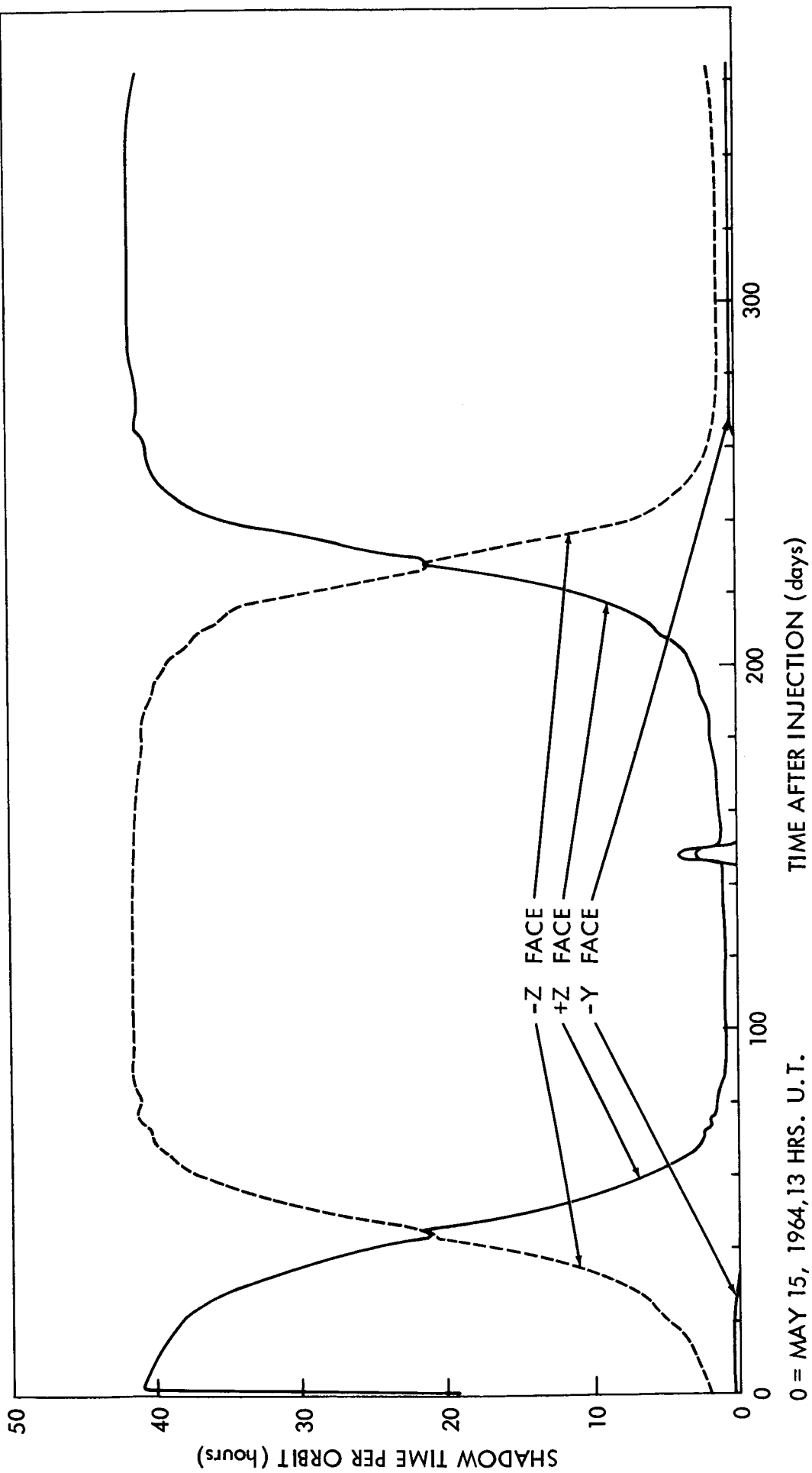


Figure 6—Main Box Shadow History

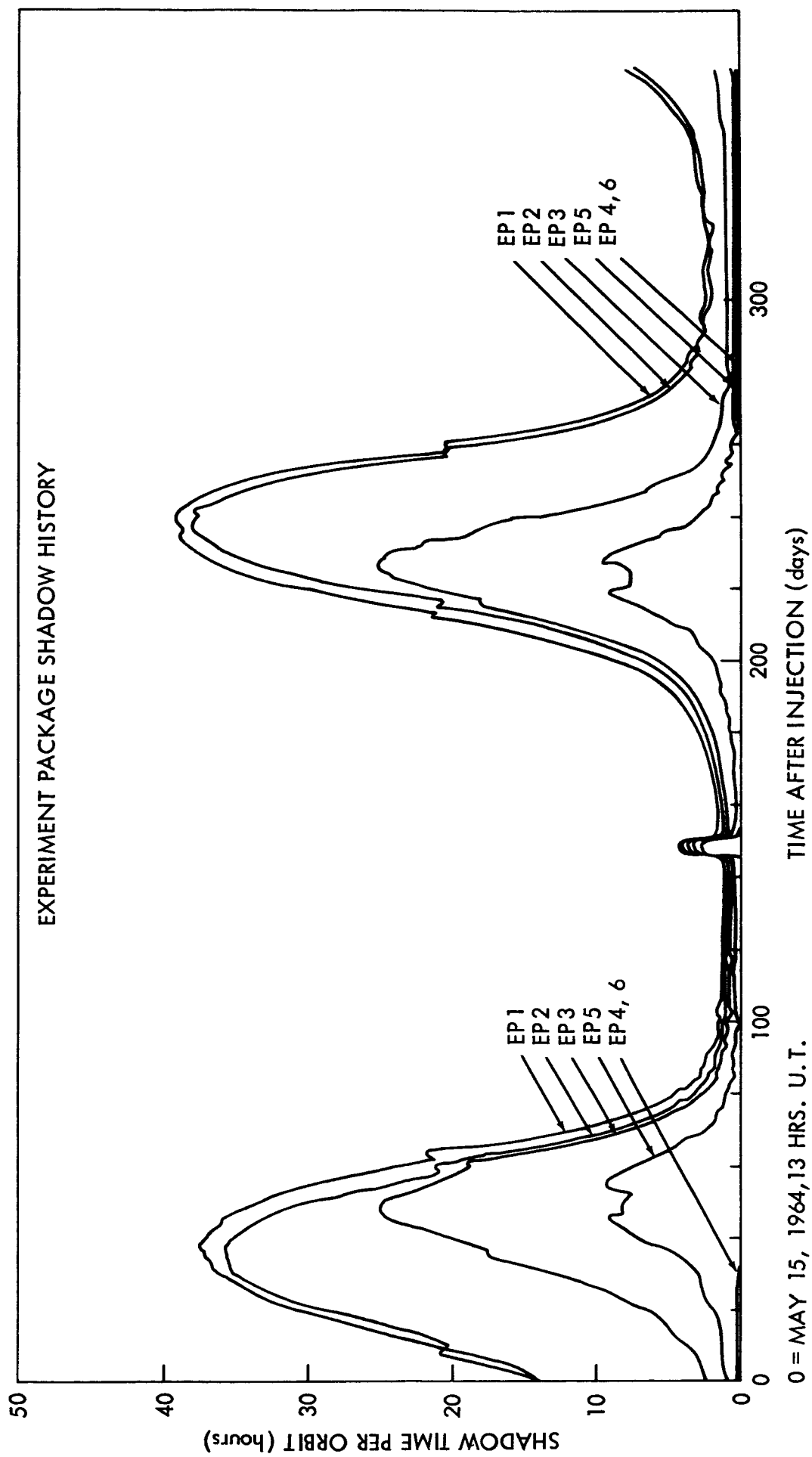


Figure 7 - Experiment Packages Shadow History

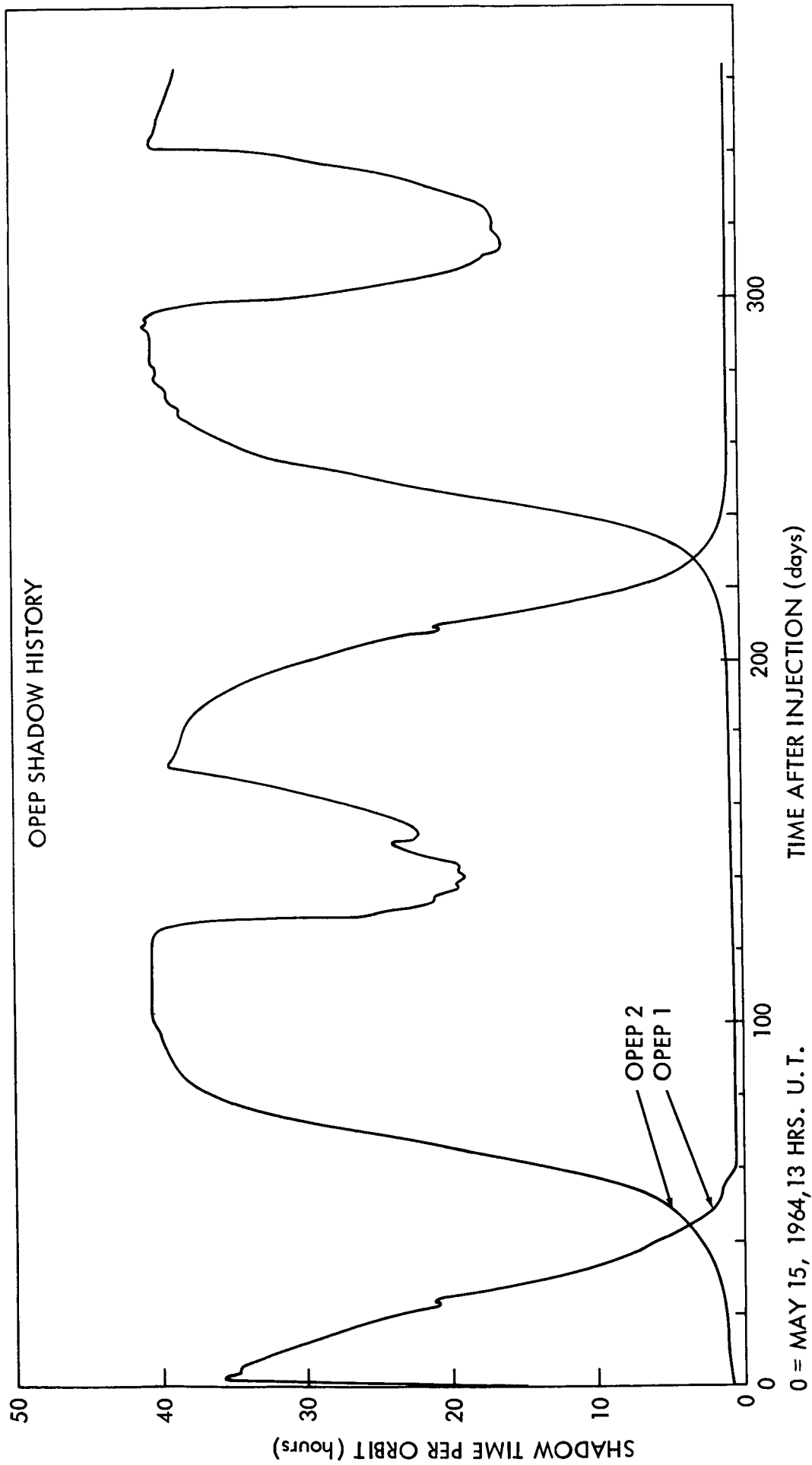


Figure 8 --OPEP Shadow History

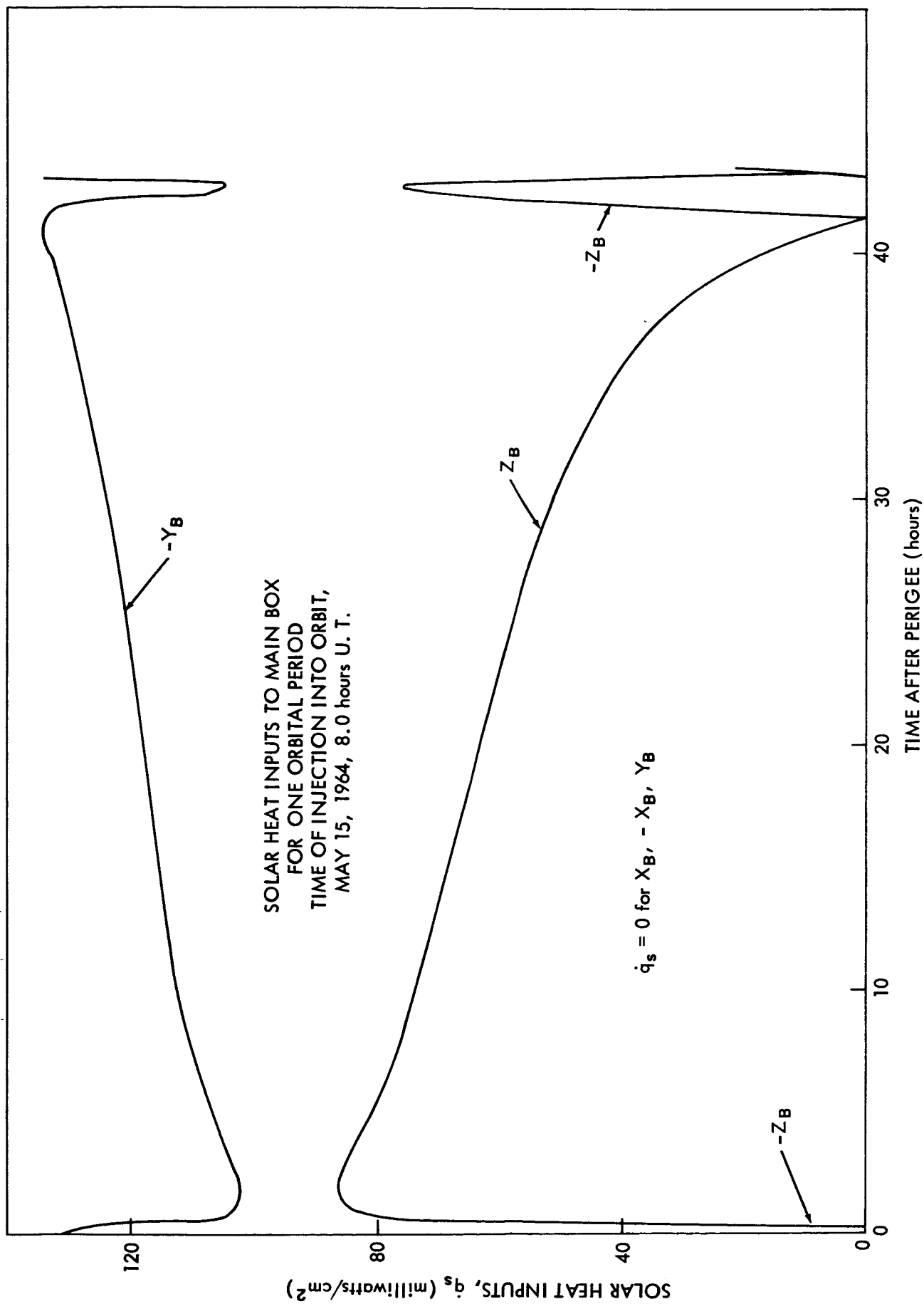


Figure 10—Solar Heat Inputs to Main Box

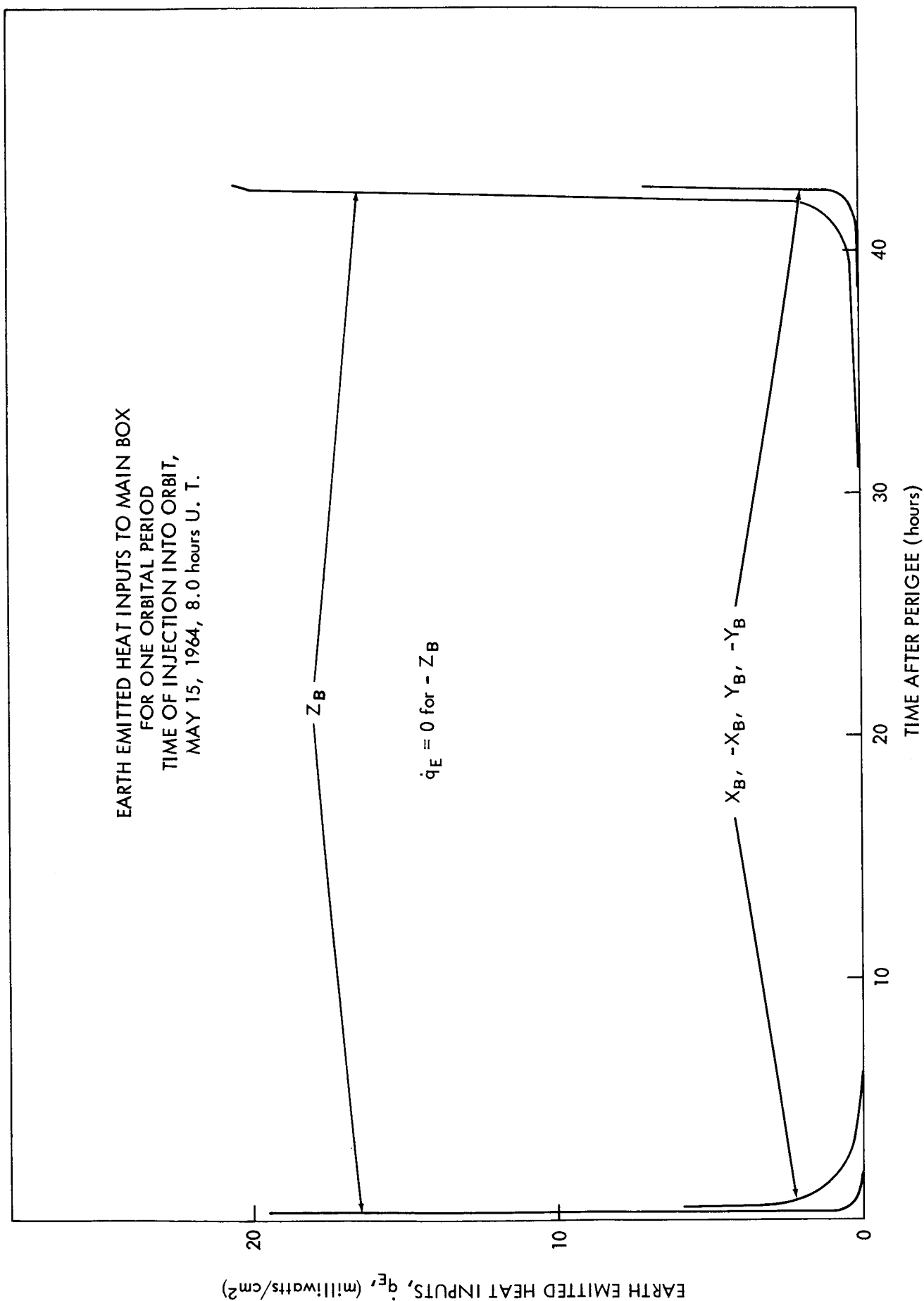


Figure 9 —Earth Emitted Heat Inputs to Main Box

SOLAR REFLECTED HEAT INPUTS
TO MAIN BOX FOR ONE ORBITAL PERIOD
TIME OF INJECTION INTO ORBIT,
MAY 15, 1964, 8.0 hours U. T.

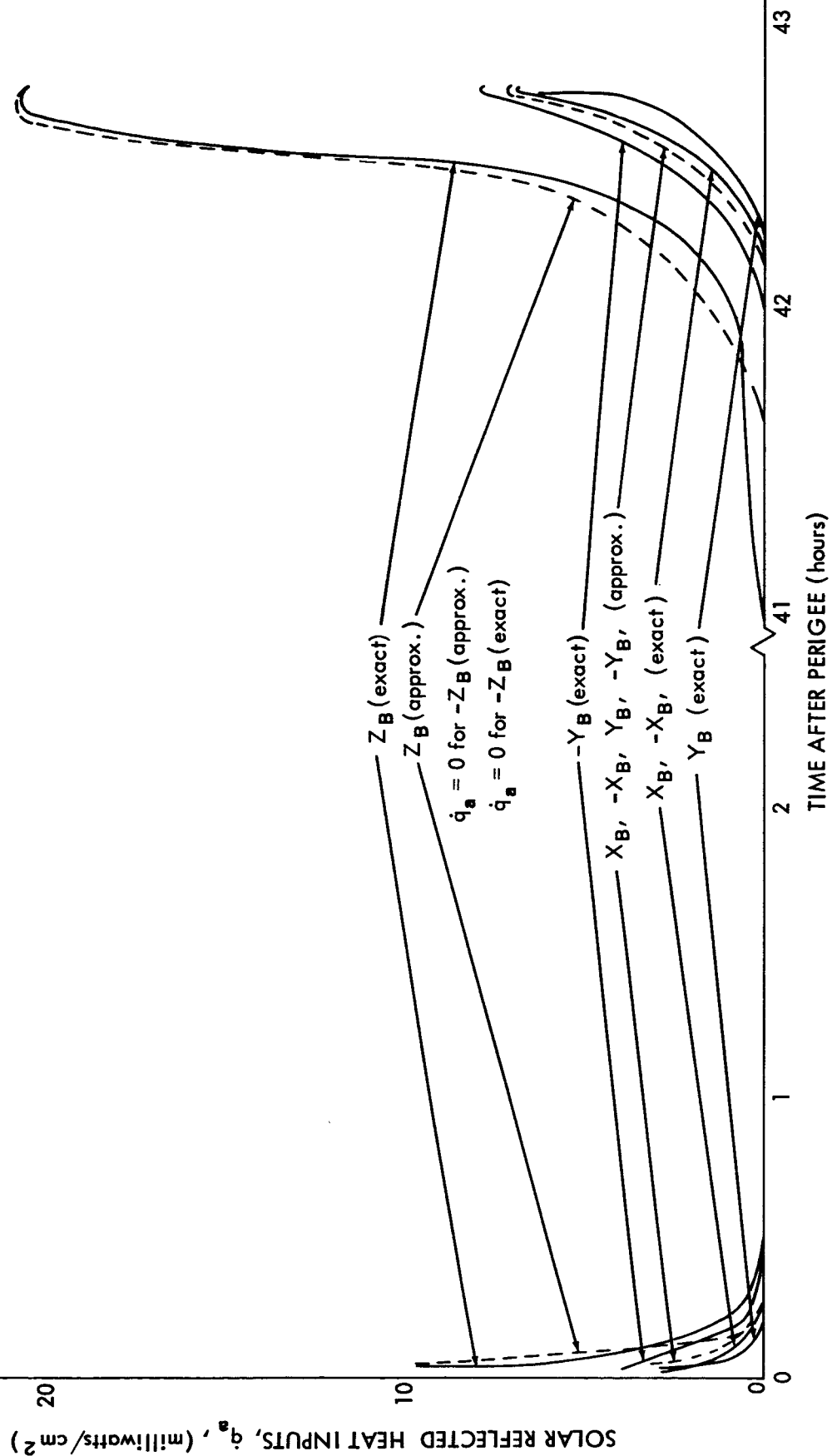


Figure 11—Solar Reflected Heat Inputs to Main Box

EARTH EMITTED HEAT INPUTS TO
BOOM-MOUNTED EXPERIMENT PACKAGES
FOR ONE ORBITAL PERIOD
TIME OF INJECTION INTO ORBIT,
MAY 15, 1964, 8.0 hours U. T.

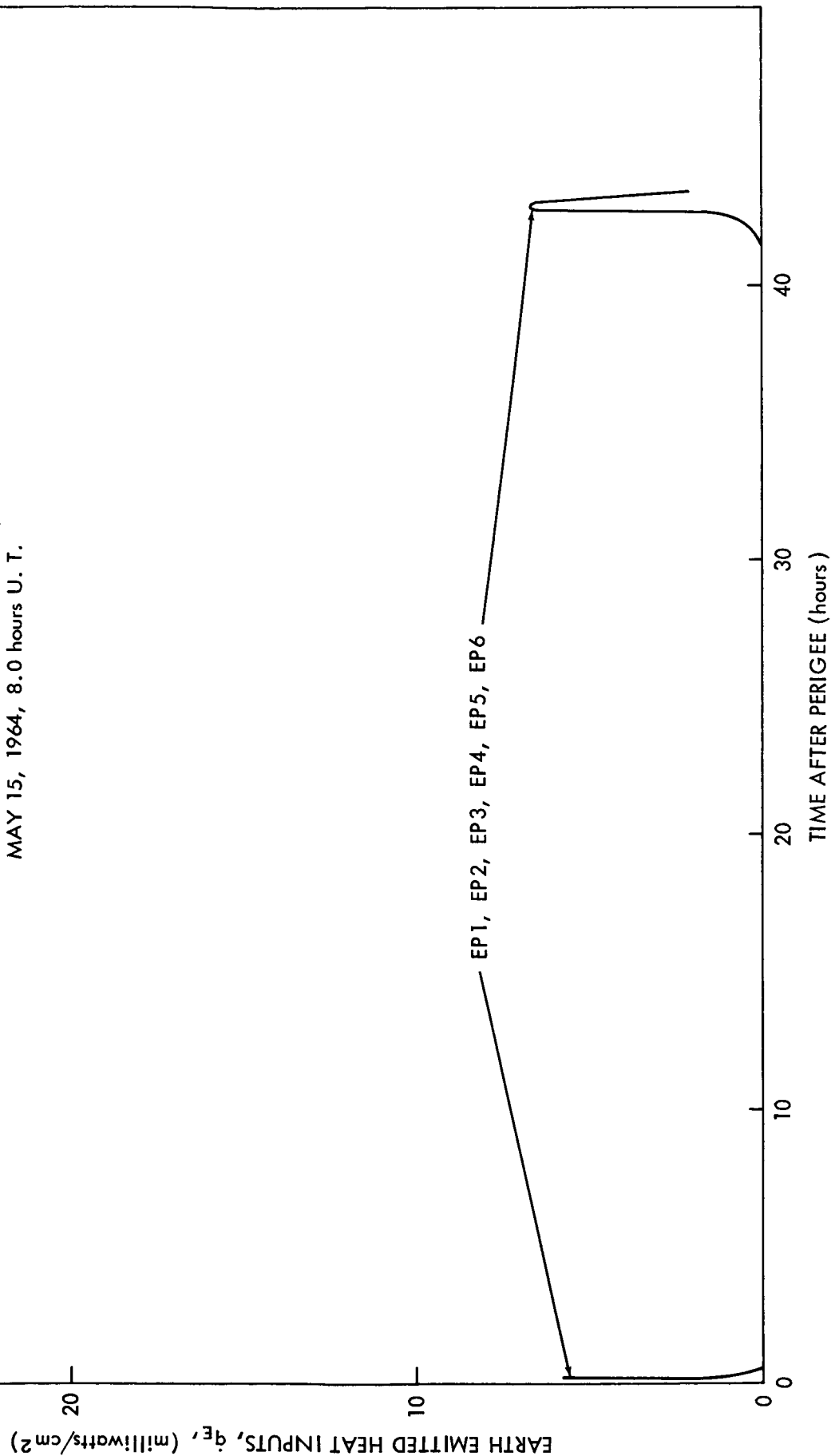


Figure 12—Earth Emitted Heat Inputs to Boom-Mounted Experiment Packages

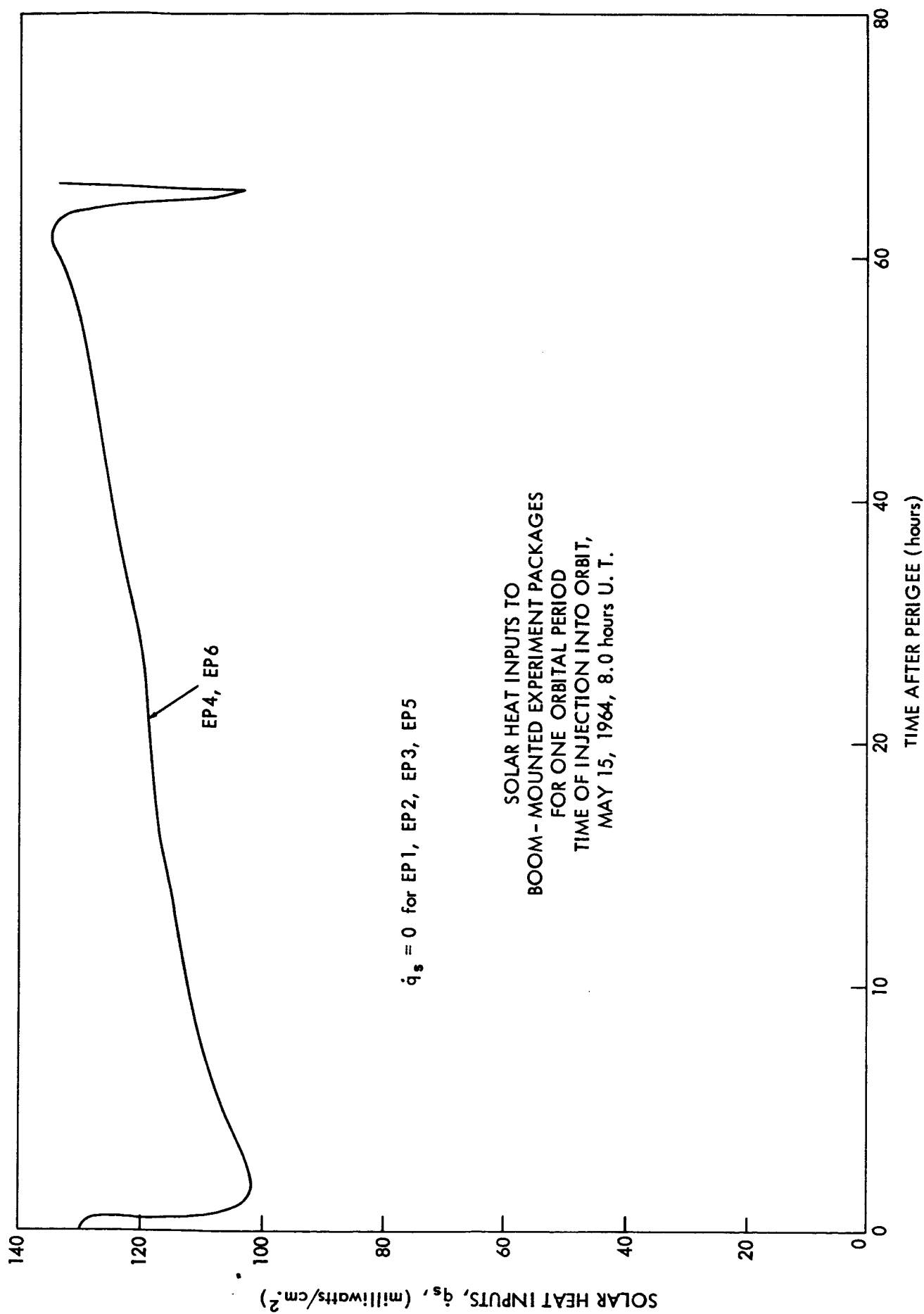


Figure 13—Solar Heat Inputs to Boom-Mounted Experiment Packages

SOLAR REFLECTED HEAT INPUTS TO
BOOM - MOUNTED EXPERIMENT PACKAGES
FOR ONE ORBITAL PERIOD
TIME OF INJECTION INTO ORBIT,
MAY 15, 1964, 8.0 hours U. T.

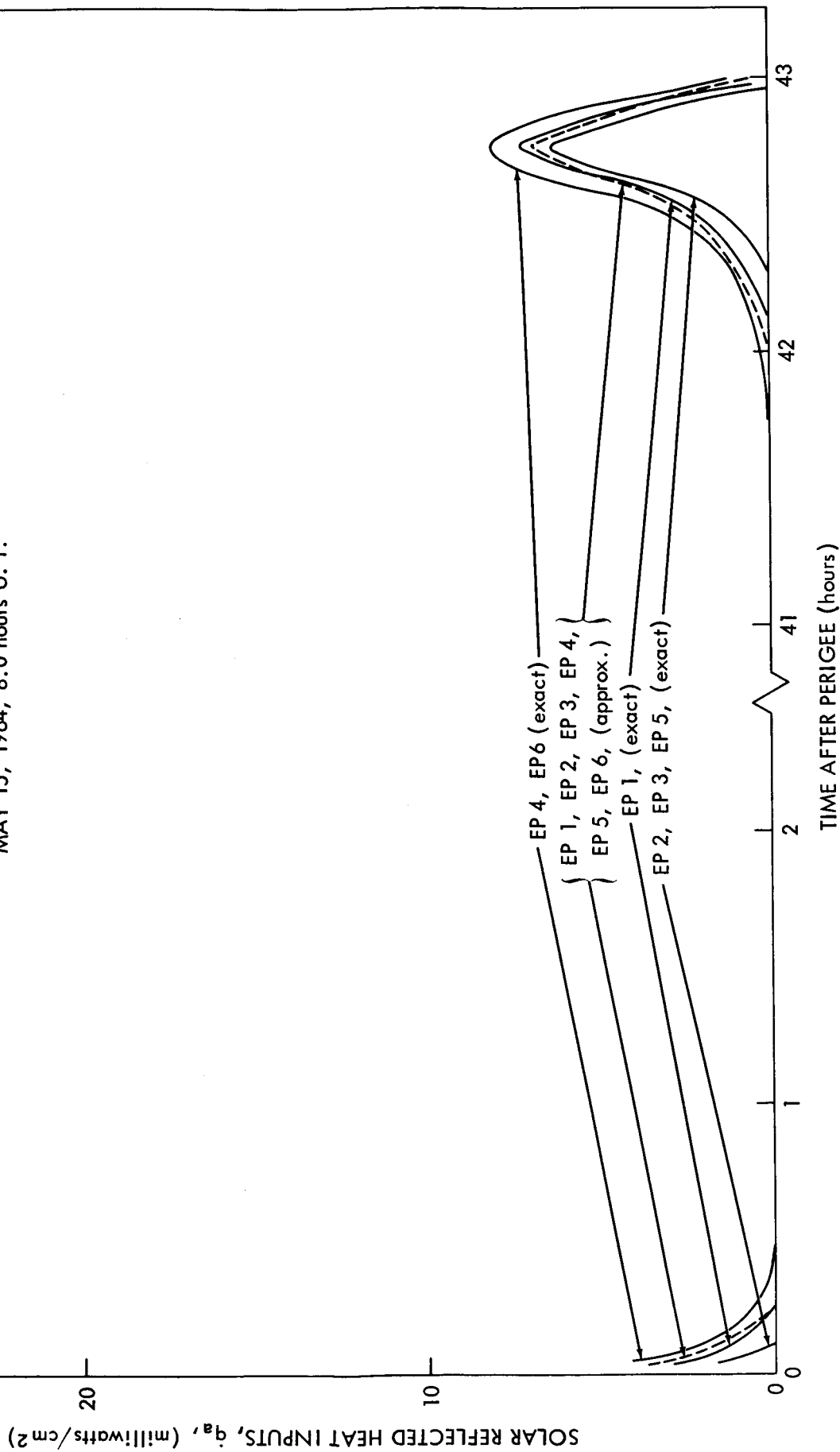


Figure 14—Solar Reflected Heat Inputs to Boom-Mounted Experiment Packages

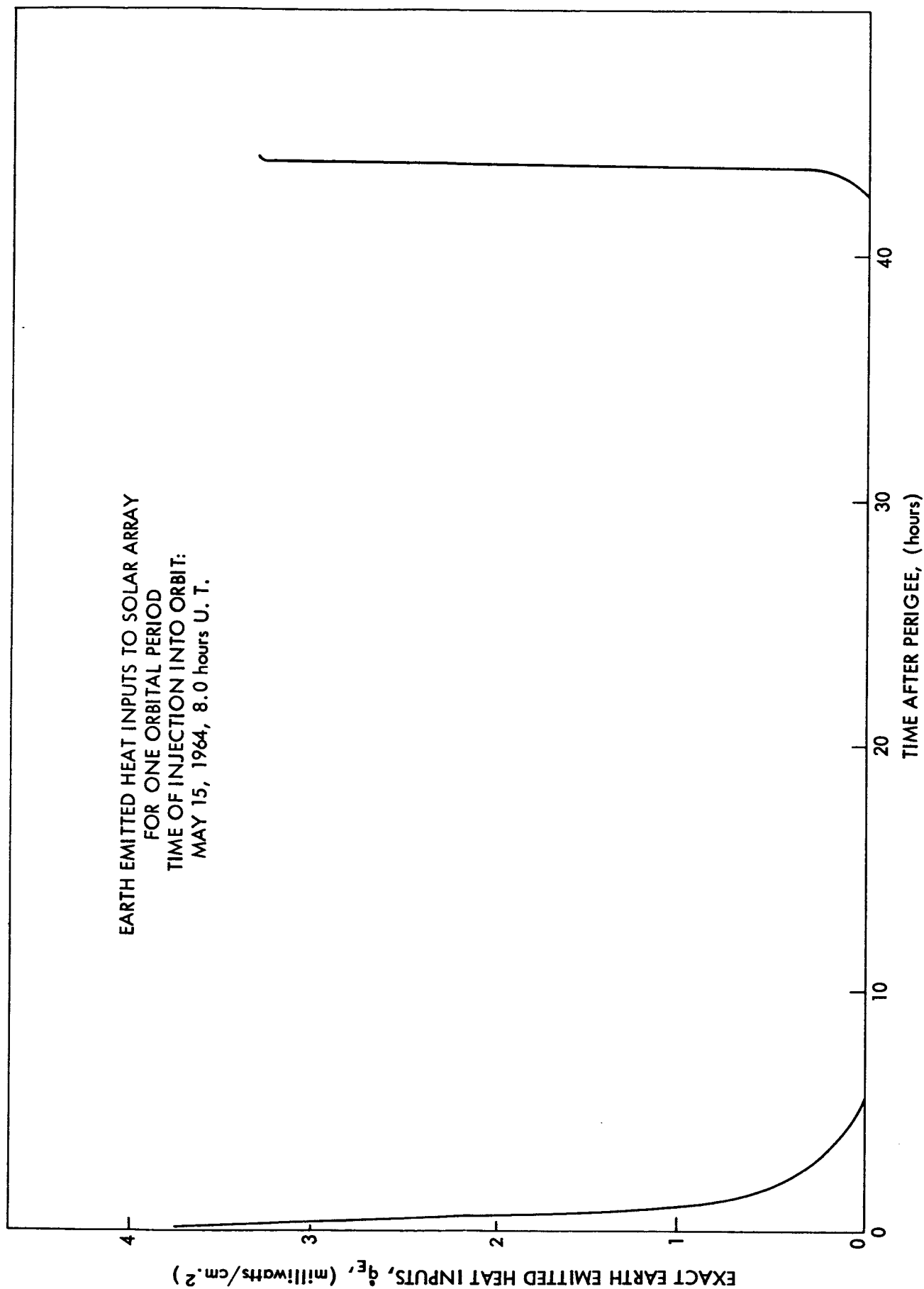


Figure 15—Earth Emitted Heat Inputs to Solar Array

SOLAR HEAT INPUTS TO SOLAR ARRAY
FOR ONE ORBITAL PERIOD
TIME OF INJECTION INTO ORBIT,
MAY 15, 1964, 8.0 hours U. T.

SOLAR HEAT INPUTS, q_s , (milliwatts/cm²)

$$\dot{q}_s = 137.4$$

TIME AFTER PERIGEE (hours)

Figure 16—Solar Heat Inputs to Solar Array

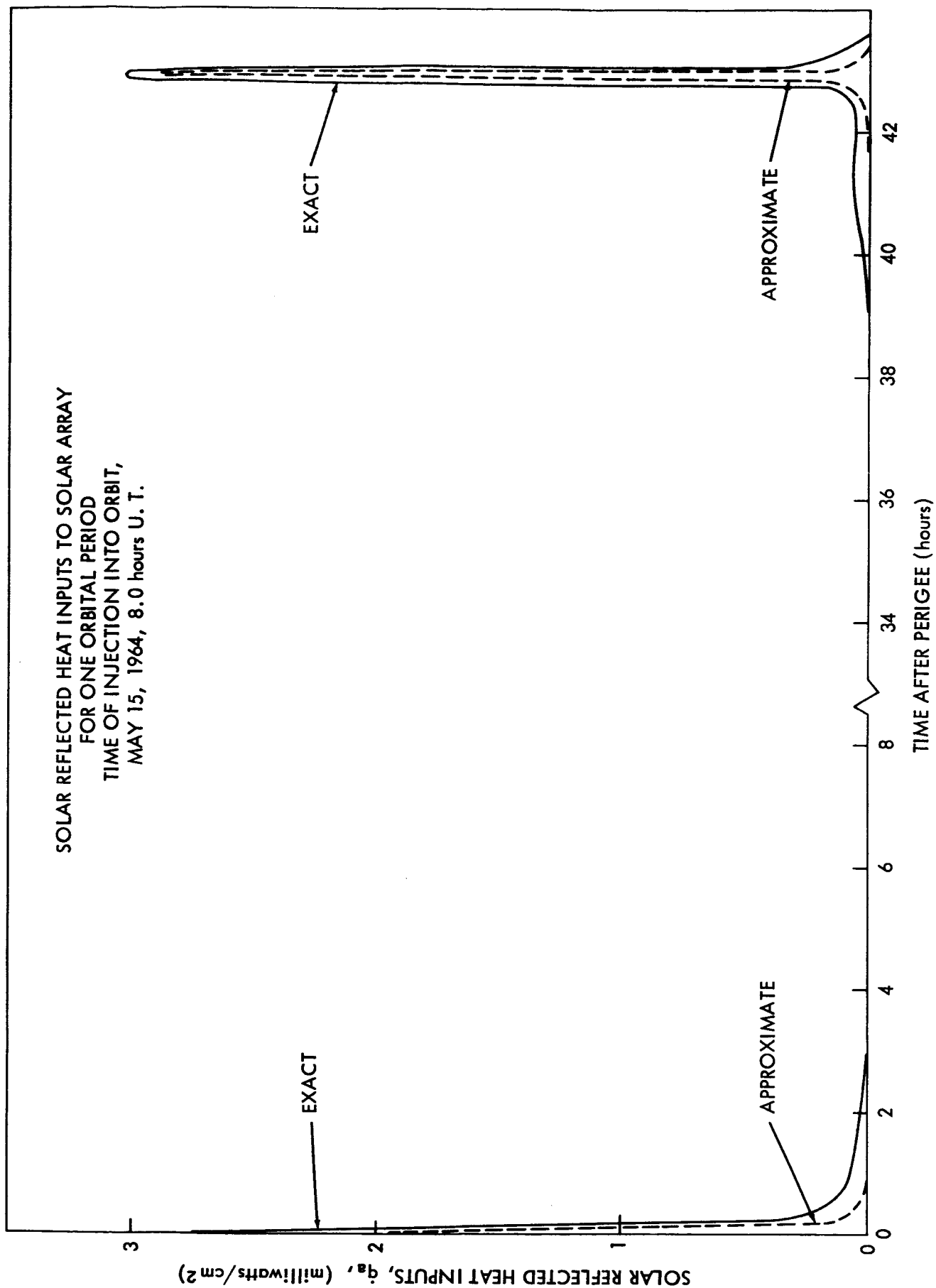


Figure 17—Solar Reflected Heat Inputs to Solar Array

EARTH EMITTED HEAT INPUTS TO OPEP
FOR ONE ORBITAL PERIOD
TIME OF INJECTION INTO ORBIT,
MAY 15, 1964, 8.0 hours U. T.

OPEP 1 AND OPEP 2

EARTH EMITTED HEAT INPUTS, q_E , (milliwatts/cm²)

TIME AFTER PERIGEE (hours)

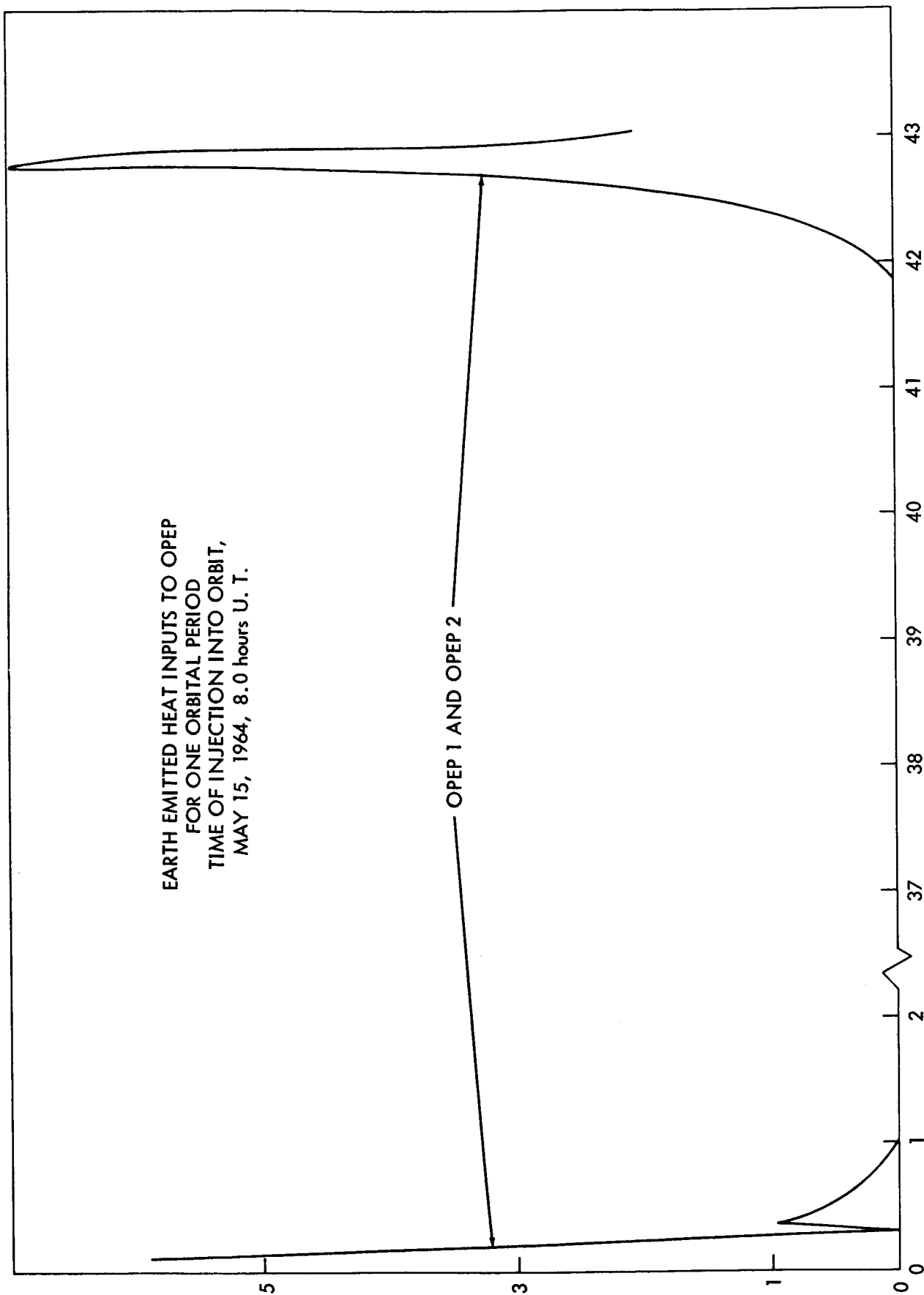


Figure 18—Earth Emitted Heat Inputs to OPEP

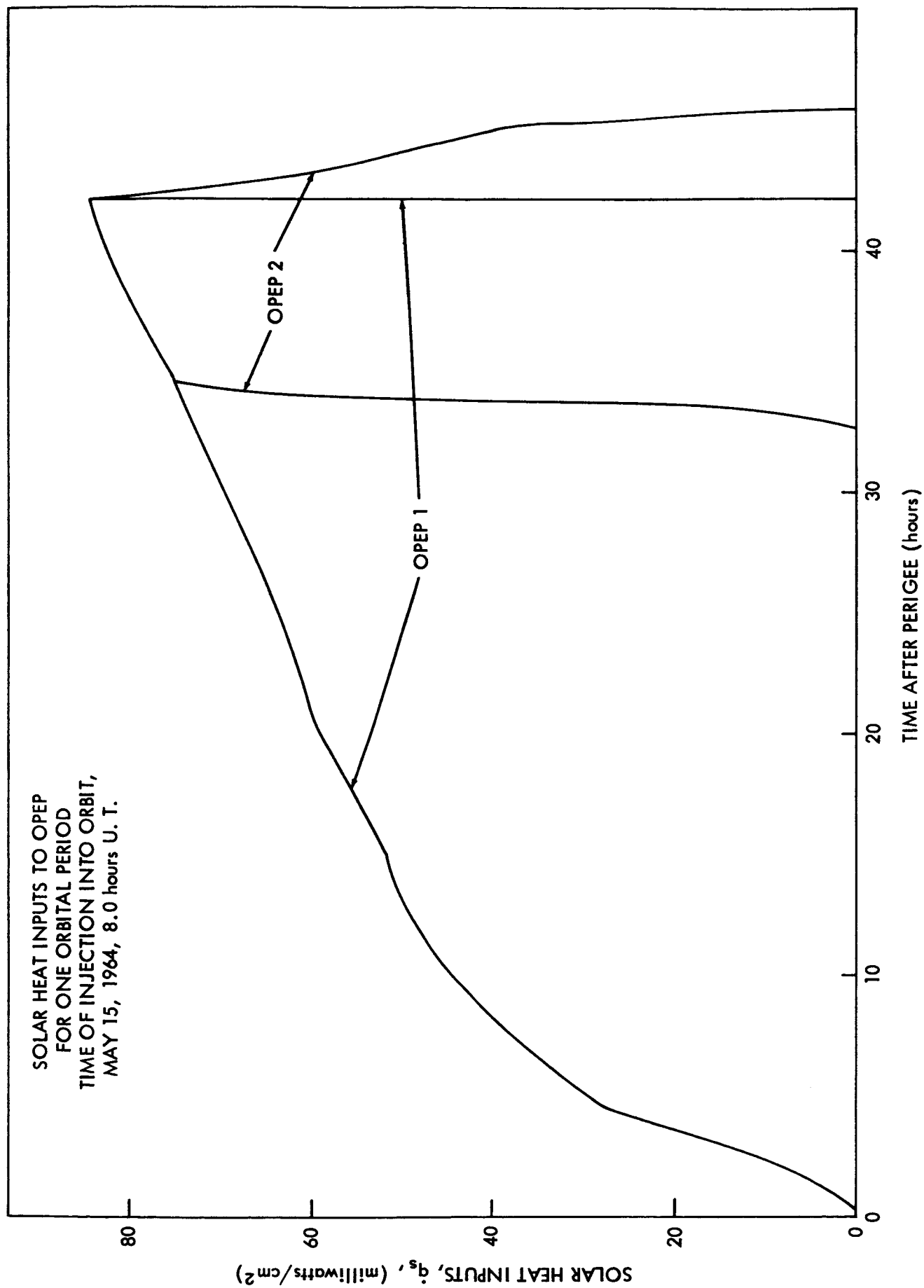


Figure 19—Solar Heat Inputs to OPEP

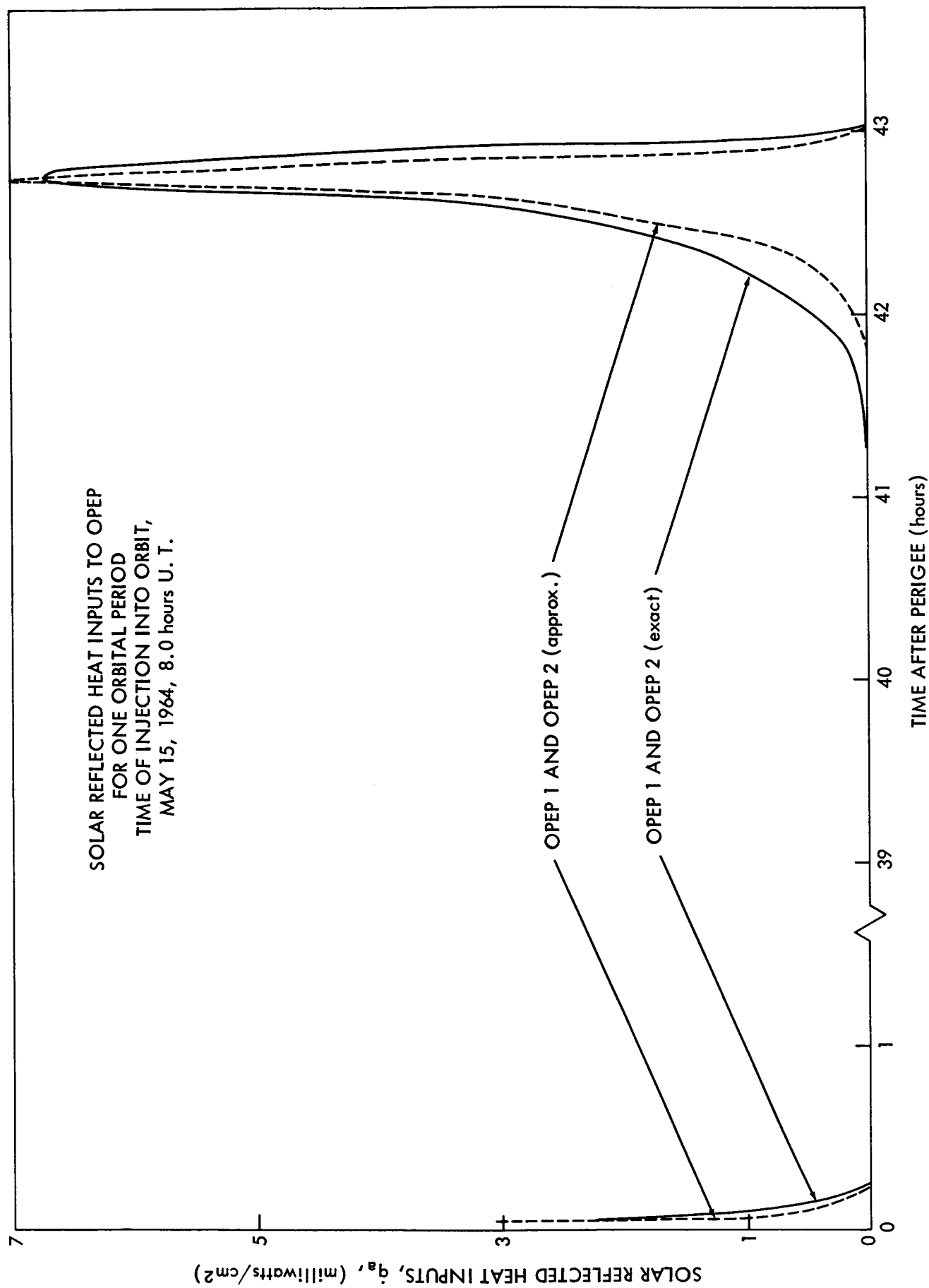


Figure 20 —Solar Reflected Heat Inputs to OPEP